République **A**lgérienne **D**émocratique et **P**opulaire
Ministère de l'**E**nseignement **S**upérieur et de la **R**echerche **S**cientifique

Université 20 août 1955-Skikda

N° : D02P2024M

Faculté des Sciences

Département de Physique

Mémoire de Master

Filière : Physique

Spécialité : Materiaux

Thème

Study of Zinc Sulphide properties for photovoltaic applications

Présenté par :
DJEFFAL Tasnim

Soutenu le: devant le jury composé de:

Zakaria HADEF	MCA	Université de Skikda	Président
Kenza KAMLI	MCA	Université de Skikda	Rapporteur
SASSANE Nacira	MRA	Centre de recherche de Annaba	Co- Rapporteur
Abdelhak FEKRACHE	MCB	Université de Skikda	Examinateur

Année Universitaire : 2023/2024

Abstract

This study focuses on the deposition and analysis of undoped and doped ZnS thin films. Our primary objective is to synthesize and analyze these films, which were deposited using the ultrasonic spray technique to optimize their properties. The initial sections of our work cover the properties and applications of ZnS, the deposition method, and fundamentals of solar cells. In the subsequent part, thin films of ZnS doped with Cd were deposited on glass substrates heated to 450 °C. These films were thoroughly characterized using various methods including XRD, spectrophotometry, and Hall effect analysis to investigate their properties.

Keywords : ZnS:Cd, Thin films, Ultrasonic spray, Doping level, Characterization.

الملخص:

تركز هذه الدراسة على ترسيب وتحليل أغشية رقيقة من ZnS غير المطعمة والمطعمة.

هدفنا الأساسي هو توضيح وتحليل هذه الأفلام، التي تم ترسيبها باستخدام تقنية الرش المهبطيلتحسين خصائصها. تتناول الأقسام الأولى من عملنا خصائص وتطبيقات ZnS، وطريقة الترسيب ،وأساسيات الخلايا الشمسية. في الجزء الأخير، تم ترسيب أفلام رقيقة من ZnS المطعمة بالكادميومعلى أسطح زجاجية مسخنة إلى 450 درجة مئوية. تم تحليل هذه الأفلام باستخدام أساليبمتنوعة بما في ذلك التشتيت بالأشعة السينية DRX، وطيفية الأشعة المرئية UV-Vis-Nir، والتحليل بتأثير هول لدراسة خصائصها .

الكلمات مفتاحية: ZnS:Cd، أغشية رقيقة ،تقنية الرش المهبطي، تطعيم، تقنيات التوصيف .

Résumé

Cette étude porte sur le dépôt et l'analyse de films minces de ZnS non dopés et dopés. Notre objectif principal est de synthétiser et d'analyser ces films, qui ont été déposés à l'aide de la technique de pulvérisation ultrasonique afin d'optimiser leurs propriétés. Les premières sections de notre travail traitent des propriétés et des applications du ZnS, de la méthode de dépôt, ainsi que des fondamentaux des cellules solaires. Dans la partie suivante, des films minces de ZnS dopés au Cd ont été déposés sur des substrats en verre chauffés à 450 °C. Ces films ont été caractérisés en profondeur à l'aide de différentes méthodes, y compris la diffraction des rayons X, la spectrophotométrie et l'analyse par effet Hall, afin d'étudier leurs propriétés.

Mots clés : ZnS:Cd, Couches minces, Spray ultrasonique, Dopage, Technique de caractérisation.

Thanks and appreciation

"In the name of Allah, The most merciful and the most beneficial"

thank God for all his blessings in completing this letter

First of all, I would like to express my deep and sincere gratitude to my supervisor, Professor Kamli Kenza for her guidance and assistance

I also extend my thanks and gratitude to my soul mate, my husband and my sweet daughter

Dedication

In the name of God, Most Gracious, Most Merciful
To the greatest in my existence
to my father, who taught me self-esteem,
diligence and perseverance to achieve my dreams,
to my mother, who was the reason for my success,
who supports me, helps me and stands by me in
all my cases. No matter what I say , I will not
fulfill their right.
To my partner, my twin soule and my generous
husband, how helps me to completed this theses, I
love you so much
To my daughter, my dear Paradise, the joy of
my life and its candle my angel, Taline Eldjana,
God made your future blossom full of joys and
successes inchallah.
To my brothers and sisters, I will not forget your
support and your love for me and for my nephews,
especially Lina, Joude and Jana

Tasnim

List of figures

Liste of tables

GENERAL INTRODUCTION

Sunlight is made up of photons or solar energy particles. These photons have varying amounts of energy corresponding to different wavelengths of the solar spectrum. A photovoltaic cell, commonly called a solar cell, converts sunlight directly into electricity.Some photovoltaic cells can also convert artificial light into electricity.

A photovoltaic cell consists of a semiconductor material. When photons hit a photoelectric cell, they may be reflected off the cell, pass through the cell, or absorbed by a semiconductor material. Only the absorbed photons provide energy to generate electricity.

This transformation discovered by the French physicist Edmond Becquerel is called 1 in 1839. It was not until 1960 that photocells found their first practical application in satellite technology. Solar panels, consisting of photovoltaic modules, began to reach the roofs of houses at the end of 1980.

because nowadays renewable energy sources, specifically wind and photovoltaics, are cheaper than conventional energies in most parts of the world. Also, compared to conventional energy sources such as coal, gas, oil and limited nuclear reserves - clean energies are just as available as the sun, hence the name "renewable energy sources". This makes it an essential element of a sustainable energy system that allows development today without risking the development of future generations .In addition, it does not emit toxic substances or pollutants into the air, which can be very harmful to the environment and humans. And its benefit lies not only in the environmental aspect, but also in the economic aspect of reducing costs.

The field of thin films is an old but very important project, it passed to numerous modifications and led to a major research effort which was undertaken in recent years in several technological fields to meet a set growing needs. [1]

Over the decades, solar panels have evolved through exciting innovations and breakthroughs. Modern, thin-film solar panels emerged as a more flexible and affordable alternative to their traditional, crystalline silicon counterparts. Their ease of installation also makes thin-film panels a desirable option among residential and commercial property owners.

Due to their numerous advantages, thin-film solar panels enjoy a wide range of applications. Thin-film panels still have a vast, open horizon filled with potential applications ahead of them, something that once seemed impossible to veterans in the solar industry.

GENERAL INTRODUCTION

The thin-film solar system's manageability and ease of maintenance draw the most attention. Below, we explore thin-film solar's many applications to reveal why people choose thin-film solar panels over other kinds of panels on the market.

Thin-film PV technologies contribute to the circular economy by providing a secondary use for mining by-products that would otherwise be disposed of. Cadmium, gallium, germanium, indium, selenium, and tellurium are sourced as by-products from the production of aluminium, zinc, lead, copper and coal. At the end of their 25+ years, useful lifetime, thin-film PV modules can be recycled to recover glass and semiconductor metals for reuse in new thin-film modules and glass products. With over 500 GW of PV installed worldwide and a probable trajectory to multi TW deployment, proven high-value PV module recycling solutions are important for all solar technologies. In addition to PV Cycle, there are several innovative high-value thin-film PV recycling initiatives operational worldwide, that are helping to close the loop.

In the last few years, metal oxides nanostructures have attracted quickly increasing attention, due to their very interesting properties .Among them, Zinc sulfide (ZnS) semiconductor is an appropriate candidate as window or buffer layer in solar cells applications.

Semiconductors have widely been used in solar cells application such us Zinc sulfide .ZnS is used in junction with SnS[2], CuO[3] and CZTS[4], it is a potential candidate to replace CdS in junction with CdTe and CIGS [5], as buffer layer or as window layer in multilayers ZnS/CdS/CdTe solar cells [4]. ZnS present many interesting properties, essentially: high transparency, large band gap, n-type conductivity and high exciton binding energy (55meV) [3]. ZnS is a nontoxic, II–VI semiconductor, with a large direct band gap of about 3.7eV. It has a refractive index (n) of 2.40 [6] which also make it suitable for application as antireflective coatings in thin-film solar cells. Different methods are used to elaborate ZnS thin films such as: Sol gel, spray pyrolysis, chemical vapor deposition, chemical bath deposition, pulsed laser and electrodeposition. The electrodeposition of thin films is considered as one of the promising ways to elaborate materials at a nanometric scale, due to its possibility of controlling thickness, processing for large-area production, low cost fabrication process and low processing temperature.

In this thesis, a characterization of a series of ZnS thin layers has been performed with different techniques such as XRD, spectrophotometer, hall effect… to evaluate the main features. ZnS thin films

deposited on a substrate by Ultrasonic Spray pyrolysis at have been studied in the analysis. And a simulation using the software SCANS was done with the results of the analysis.[4,7]

The present manuscript is divided into four chapters. The first chapters are devoted to providing a bibliographic study that provides an overview of solar cells, the principle of their operation and various types and characteristics, also we mention of some optical, electrical and structural properties of the ZnS.

a full explanation of spray pyrolysis technique used in the preparation of thin films, in addition to explaining the techniques used during their processing to reach the required results.

The third chapter dedicated to highlighting all the operating methods and used materials during the whole study. Finally, we finish this manuscript with collecting and discussing all the results obtained along this study.

GENERAL INTRODUCTION

Reference

[1] B. Rafia, caractérisation Spectroscopique des Couches minces d'oxyde de Nikel (NiO) Elaborées par Spray, doctorate thesis, Université Kasdi Merbah Ouargla, 2018.

[2] T. Miyawaki, M. Ichimura, Mater. Lett. 61 (2007) 4683–4686.

[3] L. Chabane, N. Zebbar, M. LamriZeggar, M. S. Aida, M.Kechouane, M.Trari, Mater. Sci, Effects of CuO film thickness on electrical properties of CuO/ZnO and CuO/ZnS hetero-junctions Materials Science in Semiconductor 40 (2015) 840–847 Doit :10.1016/j.mssp.2015.07.080.

[4] O.K. Echendu, A.R. Weerasinghe, D.G. Diso, F. Fauzi, I.M. Dharamadasa, Electrodeposition and Characterization of ZnS nanostructures for Solar Cells Application J. Electron. Mater Vol. 08, N°02 (2018)33-37

[5] O.K. Echendu, A. R. Weerasinghe,.G.Diso,E.Fausi,I.M.Dramadasa,J.Electron. Master 42 (2013).

[6] E. Marquez1, E. R.Shaaban, and A. M. Abousehly, New Horizons in Physics. 1(2014) 17-24

[7] A.Méndez-vilas, International Conference On Physics Chemistry and Engineering, Energy Materials & Solar Cells(SCELL-2004), 13-15 May 2004.Badajoz, Spain Vol 87(2005)747-756

Chapter I :ZnS proprieties & solar cells

In this chapter, we will report the general properties of zinc sulphide such as the formula, the structure, and its uses; similarly, solar cells will be generally described, including their components, types and technology of operation.

I.1. Zinc Sulfide

I.1.1. Chemical formula and general properties of Zinc Sulphide

Zinc sulphide (also known as zinc sulfide) is a chemical compound having the formula ZnS. This is the most common form of zinc found in nature, which is found mostly in the mineral sphalerite. The pure substance is white, and it is commonly used as a pigment, despite the fact that it is usually black due to numerous impurities. Zinc sulphide can be transparent in its thick synthetic form, and it is utilised as a window for visual and infrared opticsture.

Zinc sulphide has several properties; these are summarized in the following table:

Formula of zinc sulfide	**ZnS**
Molecular weight of zinc sulphide	97.474 g/mol
density	4.090 g/ml
Boiling point	1935 °C
Melting point	1850 °C

Table I.1 : *Properties of Zinc Sulphide* [1].

I.1.2. Structure

ZnS exists in two main crystalline forms. This dualism is an example of polymorphism. In each form, the coordination geometry at Zn and S is tetrahedral. The more stable cubic form is known also as zinc blende or sphalerite. The hexagonal form is known as the mineral wurtzite, although it also can be produced synthetically [2]. The transition from the sphalerite form to the wurtzite form occurs at around 1020 °C [2].

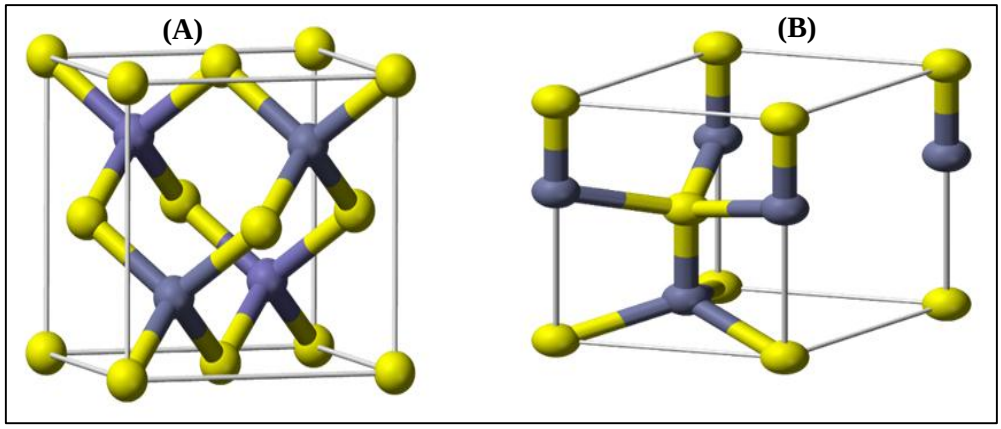

***Figure I.1**:* **(A)** *Sphalerite,* **(B)** *Wurtzite polymorph of zinc sulfide[2]*

ZnS has two available allotropic forms. One is with the hexagonal crystallographic form and it is named wurtzite. The second, more common and stable form has a cubic crystallographic structure and it is named zinc blende. The wurtzite and the zinc blende forms have band gaps of about 3.77 and 3.72 eV, respectively. The zinc blende transforms nto wurtzite at temperatures over 1052°C [3, 4]. The crystal structures of zinc sulphide are presented in **Figure.I.2**. The nanoparticles of ZnS can change their crystallographic form easier than particles in the macroscale. The zinc sulphide nanocrystals can transform from zinc the blende to wurtzite at about 400°C [3].

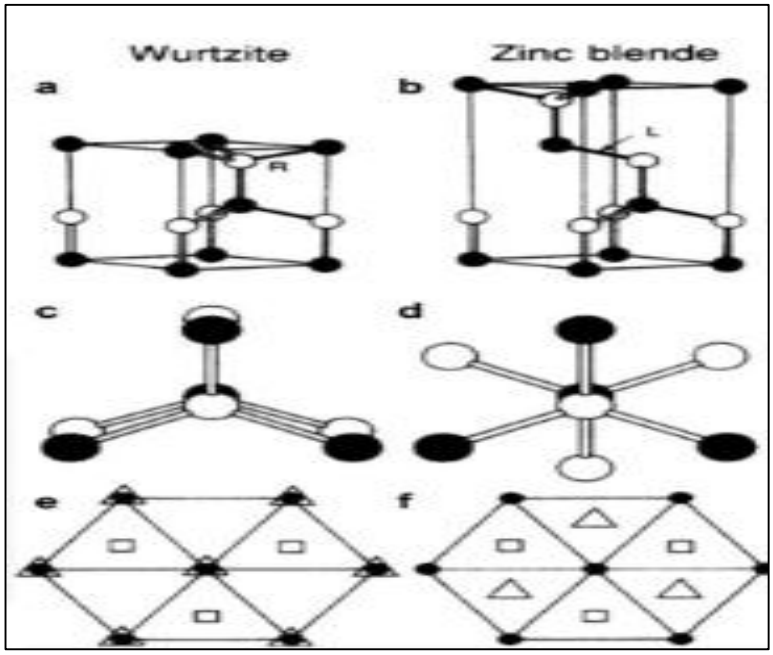

***Figure I.2** : Crystal forms of zinc sulphide* [3].

The crystal structure has an impact on the bonds energy. Between the cubic and the hexagonal form, the difference in the bond energy is about 5.6 meV/atom. For one-dimensional nanoparticles, the diameter has an influence on the bond's energy. The energy bond decreases with the increase of the nanoparticle's diameter. This phenomenon is observed only for the material that is in the nanoscale. For the bulk material, the diameter has no impact to the value of the bond's energy [5]. In **Figure.I.3**, the influence of diameter on the bond's energy is depicted. For the bulk material, the bonds energy is stable for different diameters in contrast to ZnS nanowires. For the lower values of crystal diameters, the bond's energy is higher. The difference in the bond energy between cubic and hexagonal forms is also depicted [5].

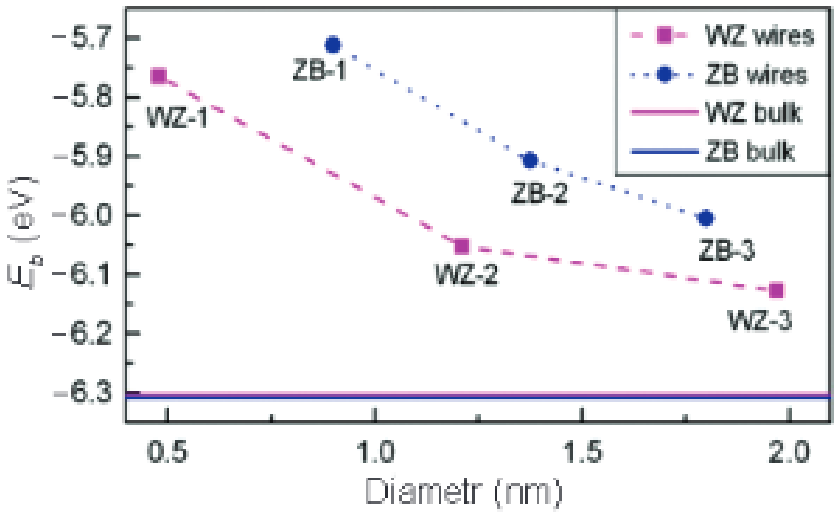

Figure I.3 : *The influence of diameters ZnS nanowires on bonds energy [5].*

I.1.3. Physical Properties of ZnS

Zinc is typically found in larger, more complicated minerals. When secluded, it is an extremely gleaming, whitish-blue metal. The metal is less soft than copper and has fewer uses [6].

PROPERTY	ZnS	
	ZINC BLENDE	WURTZITE
Lattttice parameters at (300k)	a = 0.541 nm	a = 0.3811 nm c = 0.6234 nm
Density (at 300k)	4.11 $g.cm^{-3}$	3.98 $g.cm^{-3}$
Dielectric constant	8.9	9.6
Refractive index	2.368	2.356 / 2.378
Energy Gap Eg (at 300k)	3.68	3.91
Exciton binding enery (meV)	39	39
Position of UV emissions	330 - 345nm	330 - 345nm

Table I.2 : *Physical properties of fundamental ZnS structure [1].*

I.1.4. Optical properties

Zinc sulfide has a high refractive index of about 2.35 at wavelength of 632 nm **[7]**, **Figure I.4** *(a)* and *(b)* show the transmittance and the absorbance, respectively, of ZnS thin films deposited by Successive Ionic Layer Adsorption and Reaction (SILAR) at different annealing temperatures. The absorbance is low in the visible and near infrared regions, but is high in the UV region, with an enhanced absorption observed close to 360 nm. The transmittance is very high in the visible and near infrared regions, and low in the UV region. The high transmittance of about 90 % in the visible range show in **Figure I.4** *(a)* leads to the conclusion that the ZnS films are actually efficient transmitting and antireflective materials. **Figure I.5** *(a)* shows the plot of $(\alpha h\nu)^2$ (where α is the optical absorption coefficient and $h\nu$ is the energy of the incident photon) as a function of the photon energy. **Figure I.5** *(b)* shows the energy gap as a function of the temperature. The decrease in energy gap with increasing annealing temperature could be attributed to improvement in the crystal quality or to possible variation of the grain size [7].

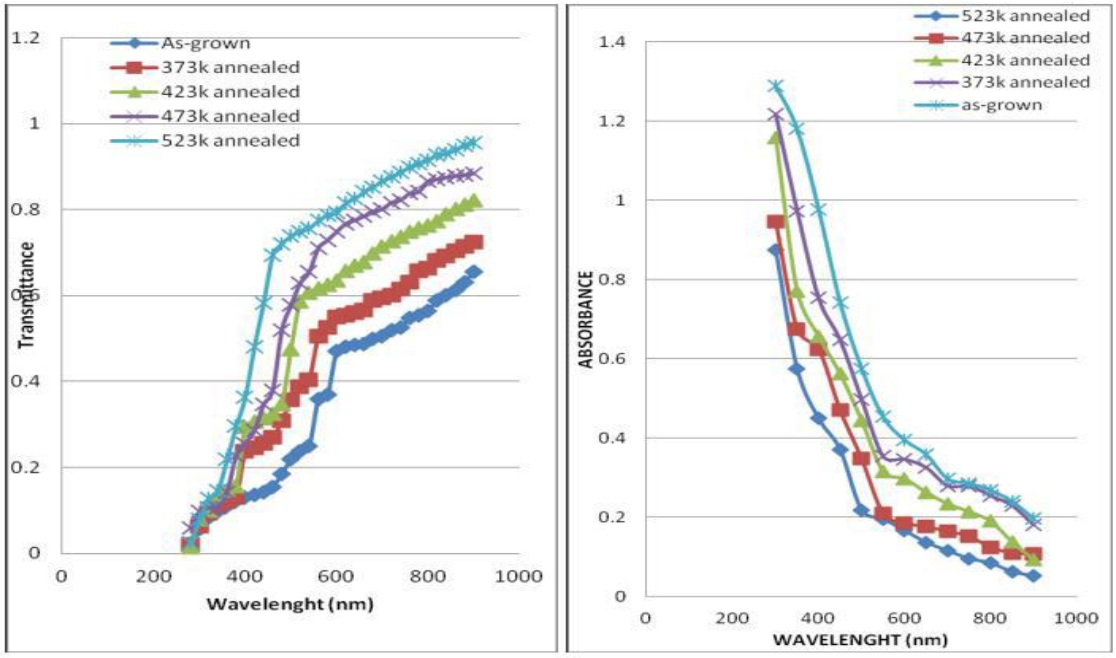

Figure I.4 : *Transmittance (a) and absorbance (b) versus the wavelength for ZnS layers [7].*

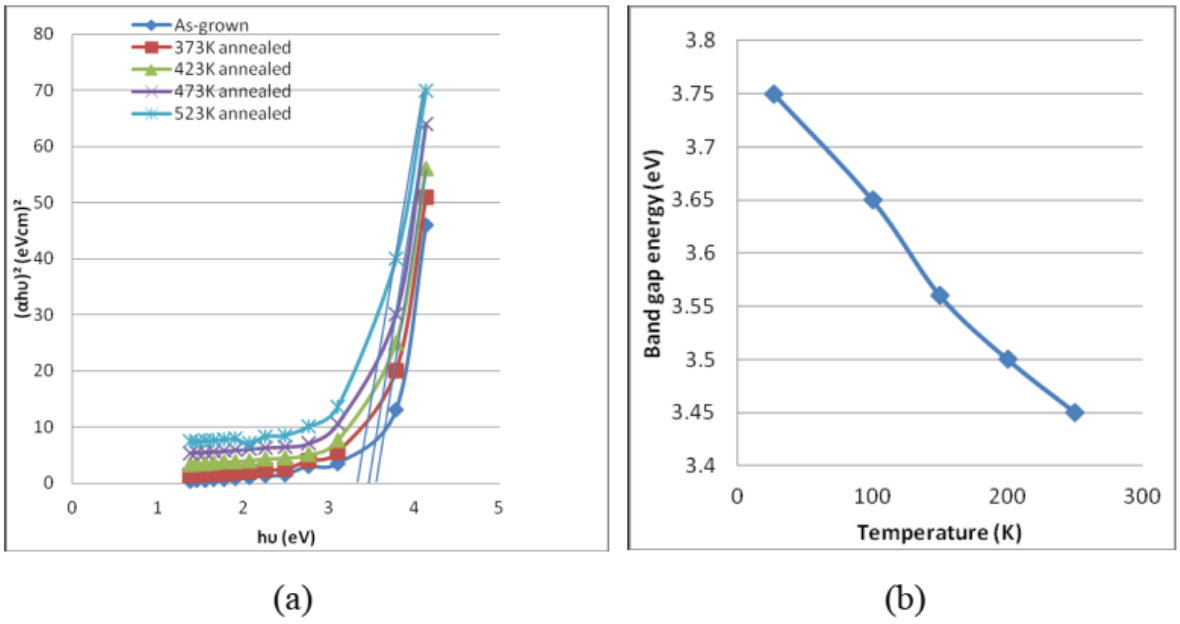

Figure I.5 : *$(\alpha h\nu)^2$ as a function of the photon energy (a) and energy gap as a function of temperature (b) for ZnS layers [7].*

I.1.5. Photo- and electroluminescence of ZnS

ZnS is well known for its photoluminescence (PL) and electroluminescence (EL). ZnS- based phosphors exhibit excellent conversion efficiencies for fast electrons into electron- hole pairs [9]. The

PL properties of ZnS (1D) nanocrystals in most cases depend on their shape or size, but for example for nanowires and nanoribbons, they are very similar. The PL measurement of both structures of ZnS at room temperature shows strong and broad emission spectra with the maximum centred at 398 nm [9]. Generally, the 1D ZnS nanoparticles have a strong green emission band, centred at about 530–540 nm, and a weaker blue emission band, centred at about 440 nm [3]. The electroluminescence process is defined as non-thermal generation of light through the application of an electric field to the sample. Zinc sulphide is one of the best semiconducting functional materials for EL devices [10]. The temperature has a strong influence on the electroluminescence in ZnS. With an increase in the temperature, the EL brightness increases. The nanoparticles of ZnS also have a promising electroluminescence properties. They are used in semiconductor-based light emitting diodes (LEDs). The highly saturated colour emission could be obtained in such devices based on ZnS nanoparticles [3]. The ZnS nanoparticles are often dotted with another metal in order to improve their EL properties. Dotted ZnS nanocrystals have a high quantum efficiency with narrow emission and broad excitation spectra [11].

I.1.6. Applications of ZnS

I.1.6.1. Luminescent Material

With a few ppm of sufficient activator, zinc sulphide exhibits intense phosphorescence (first observed by Nikola Tesla in 1893)[13] and is now employed in a variety of applications, ranging from cathode ray tubes to X-ray displays to glow in the dark items. The colour produced when silver is used as an activator is a vivid blue, with a maximum wavelength of 450 nanometers. Manganese produces an orange-red colour with a wavelength of roughly 590 nanometers.Copper has a long-lasting glow and a characteristic greenish glow-in-the-dark appearance. Electroluminescent panels also use copper-doped zinc sulphide ("ZnS + Cu"). When illuminated with blue or ultraviolet light, it also exhibits phosphorescence due to impurities.[13]

I.1.6.2. Optical Material

Zinc sulphide is also employed as an infrared optical material since it transmits wavelengths from visible to little over 12 micrometres. It can be moulded into a lens or utilised planar as an optical window. It's manufactured as microcrystalline sheets from hydrogen sulphide gas and zinc vapour, and it's marketed as FLIR-grade (Forward Looking Infrared) since the zinc sulphide is milky-yellow and opaque. When this substance is hot isostatically pressed (HIPed), it can be transformed to Cleartran, a water-clear form (trademark). Irtran-2 was the name given to the first commercial versions, however, that name is no longer used [13].

I.1.6.3. Catalyst

When illuminated, fine ZnS powder acts as a photocatalyst, producing hydrogen gas from water. During the production of ZnS, sulphur vacancies can be added, which gradually changes the white-yellowish ZnS into a brown powder and increases photocatalytic activity by increasing light absorption [14].

I.1.6.4. Applications of ZnS nanocrystals – optoelectronic devices

ZnS nanocrystal semiconductors are one of the most interesting and important groups of compounds used in electronic and optoelectronic devices. The development of these materials is one of the most important trends in this field [15]. 1D nanocrystals can be used in Field-Effect Transistors (FETs). He et al. fabricated FET based on ZnS/SiO2 core/shell nanocables. For the fabrication of FETs, the synthesised ZnS/ silica nanocables were transferred from the Si substrate to Au/Ti electrodes. In order to Firmly contact the Au/Ti metal electrodes and ZnS core of the nanocable, focused ion beam microscopy was used to cut the nanocable at the two ends of exposed ZnS core. Then, a Pt mixture was deposited at the ends in order to make contacts between the ZnS core and Au/ Ti electrodes .The typical FET is a three terminal device. The names of terminals refer to their function and they are called: gate, drain and source. The gate terminal controls the opening and closing of the physical gate with permits or blocks of electron flow by creating or eliminating conductive the channel between drain and source [15]. An example of FET is presented in **Figure. I.6.** The grey balls in Figure 4 illustrate the crystals of the semiconductor.

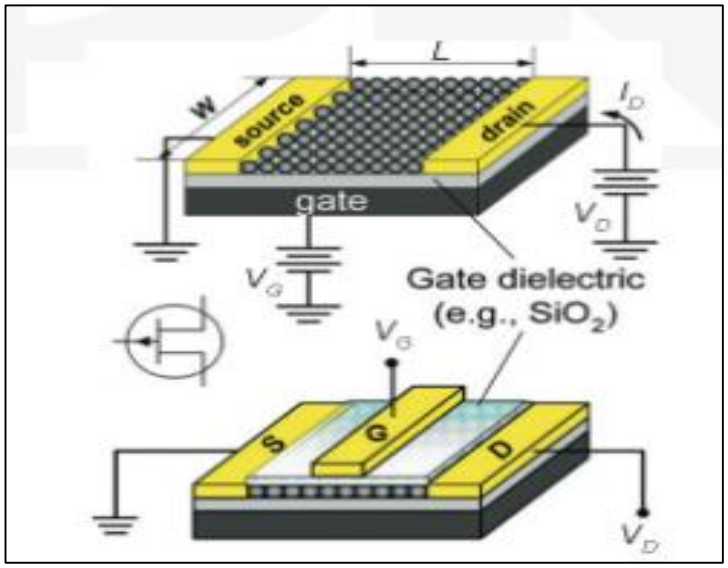

***Figure I.6** : Typical bottom-gated (a) and top-gated (b) of Field-Effect Transistors [15]*

I.1.6.5. Solar Cells

Zinc sulfide (ZnS) may be a semiconductor with a large bandgap that demonstrates several attention-grabbing phenomena, like size-induced absorption and visible lightweight emission, a short radiative time, etc. ZnS is one in every of the foremost studied host lattice within the field of phosphor technology. Advances in ZnS chemistry have recently shown the possibility that this material may well be proven effective for several potential applications if the scale of the material is reduced to nano-regime. It's renowned that once the electronic wave functions are affected by the scale limits, the development of quantum confinement happens. In many analysis areas, like semiconductors, optoelectronics, and solar cells, the longer-term applications of quantum-confined ZnS are expected to dominate material production within the next decade. As of now, size-controlled ZnS has been successfully synthesized by several wet-chemical techniques. Sadly, the applying of ZnS material for photovoltaic cell application is feebly explored [16].

I.2. Solar cells

I.2.1 Solar spectrum

The study of solar cells (progress, optimization and characterization….etc.) need some information about the source of energy used; the sun. This star is the biggest member of the solar system. The sun is a big sphere of plasma composed of *H* and *He* and some small amounts of other elements, it has an effective black-body temperature *TS* of *5777 K*. The diameter of the sun is around 1.39x109 m and the distance between it and the earth is about 1.5x1011 m. The solar radiation is partially absorbed and scattered by its passage through the atmosphere. The absorption of the *X*–rays and extreme ultraviolet radiations of the sun is principally caused by nitrogen and oxygen while the absorption of the ultraviolet (λ<0.40 μm*) and infrared radiations (*λ>*2.3* μm) is mainly caused by the ozone and water vapors. The atmosphere of the earth absorbs the ultraviolet (*UV*) and far infrared radiation and allows only short wavelength radiation (i.e. between *0.29* μm *and 2.3* μm). It does not permit radiation having wavelength λ>*2.3* μm, (i.e. long wavelength radiation) [17].

The wavelength distribution of the sunlight (power per unit area and per unit wavelength) follows approximately the radiation distribution of a black body at this temperature as shown in **Figure I.7**. The total energy per unit area integrated over the entire spectrum and measured outside the atmosphere perpendicular to the direction of the sun is essentially constant. This radiation power is referred to as the solar constant or air mass zero (AM0) radiation [18]. Outside the atmosphere the spectrum is *AM0* and that on the surface of the earth for normal incidence is *AM1* [19].

$$AM = 1/\cos(\theta) \quad \text{(II.1)}$$

The θ represents the angle of the sun to the vertical [18].

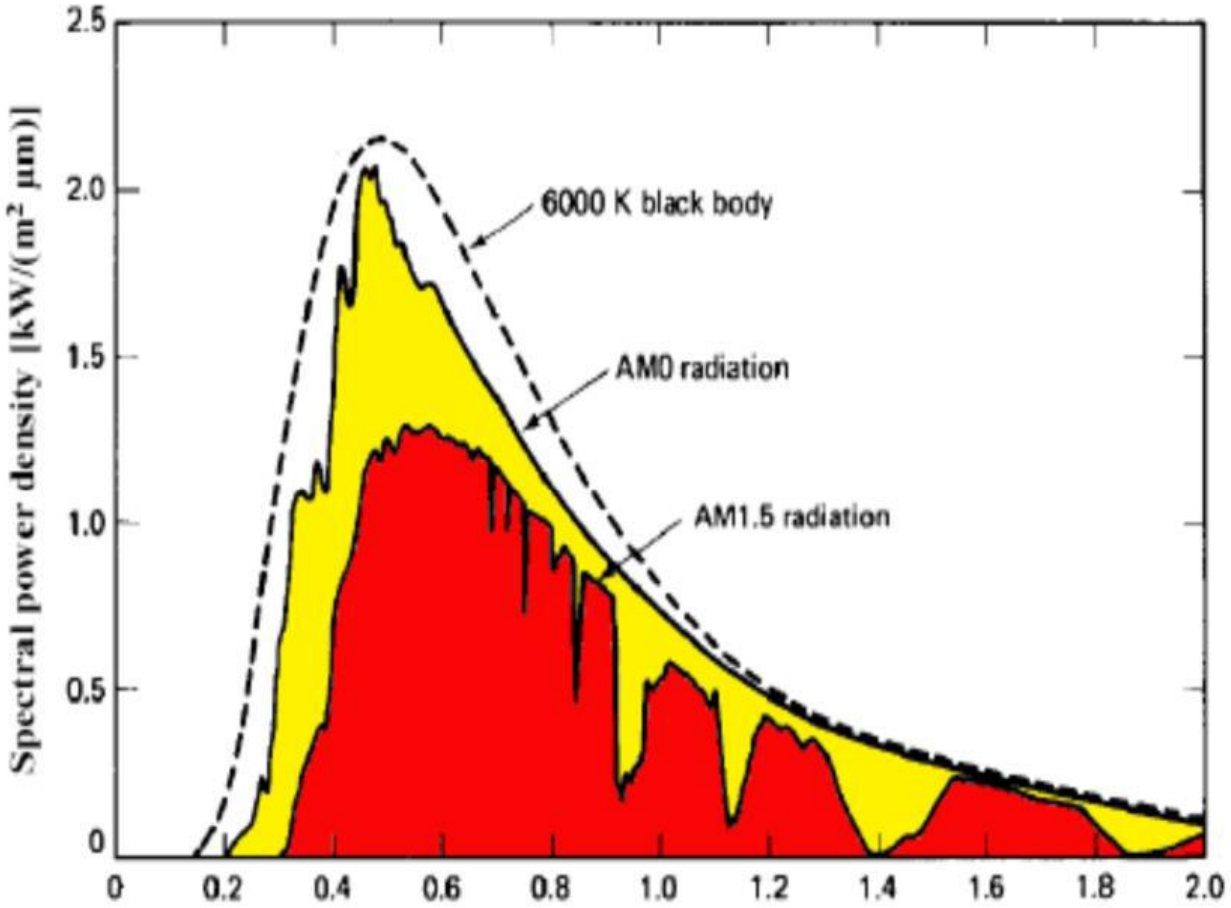

Figure I.7 : *Spectral power density of sunlight showing AM0 (extraterrestrial radiation), AM1.5 (terrestrial) and the black body radiation at 6000 K [20]*

I.2.2. Solar Radiation

When the solar radiation passes through the earth's atmosphere, the spectral distribution is attenuated and changed as a result of absorption and scattering phenomena in the gas, water and dust. Atmospheric absorption is commonly caused by ozone (O3), oxygen (O2), nitrogen (N2), carbon dioxide (CO2), carbon oxide (CO) and water vapour (H2O) while scattering is mostly caused by aerosols, air molecules (Rayleigh scattering), dust and water droplets **Figure I.8.** [21].

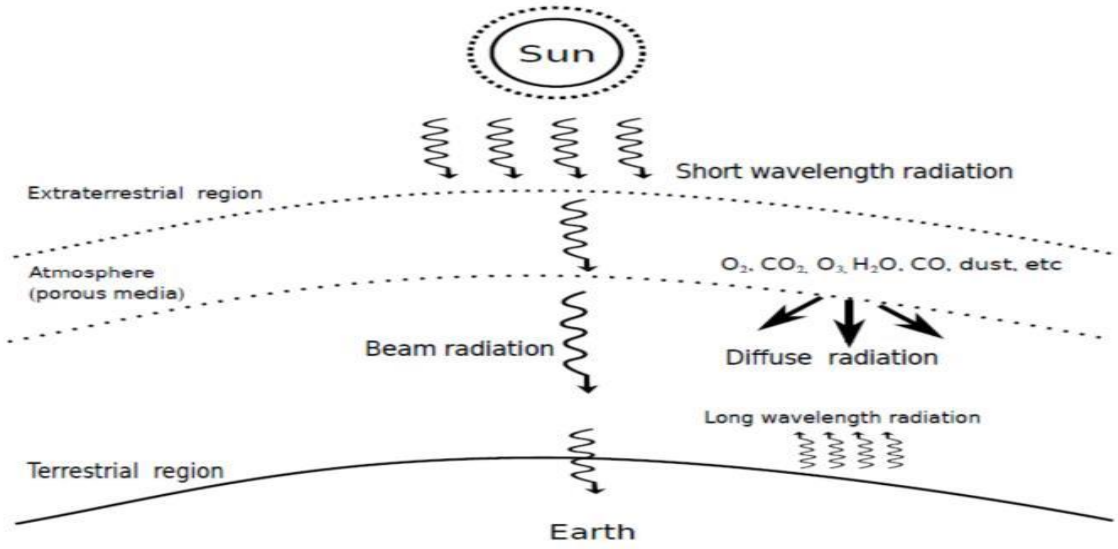

***Figure I.8**. Terrestrial, extra-terrestrial regions and atmospheric effects [21].*

I.2.3. Solar Cell

A solar cell (also known as a photovoltaic cell or PV cell) is defined as an electrical. device that converts light energy into electrical energy through the photovoltaic effect. A solar cell is basically a p-n junction diode. Solar cells are a form of photoelectric cell, defined as a device whose electrical characteristics – such as current, voltage, or resistance – vary when exposed to light. Individual solar cells can be combined to form modules commonly known as solar panels. The common single junction silicon solar cell can produce a maximum opencircuit voltage of approximately 0.5 to 0.6 volts. By itself this isn't much – but remember these solar cells are tiny. When combined into a large solar panel, considerable amounts of renewable energy can be generated [22].

I.2.3.1. Structure of solar cells

During the made of a silicon solar cells single crystal wafers, polycrystalline wafers or thin films are using. Single crystal wafers are shred, (about 1/3 to 1/2 of a millimeter thick), from a large single crystal bullion which has been stretched out at around 1400 °C, which is a very expensive process. The silicon must be of a very high purity and have a near perfect crystal structure so it can be absorb the sunlight [22].

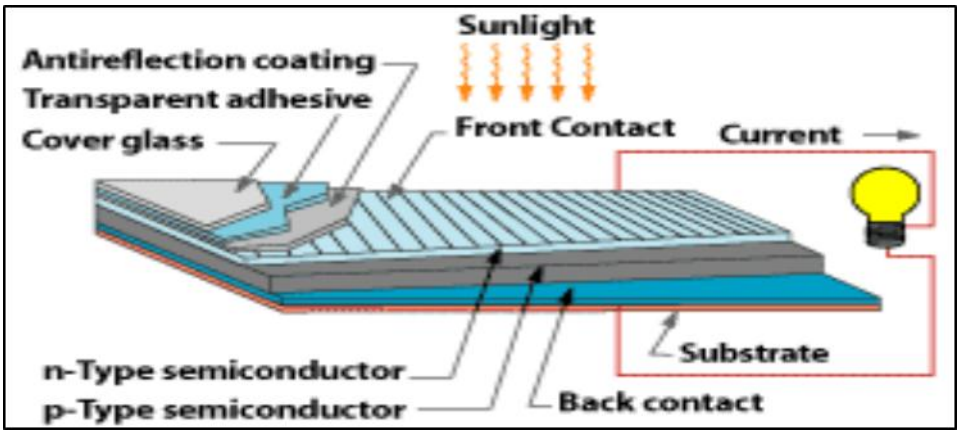

Figure I.9 : *Schematic of a typical solar cell [24]*

Crystalline silicon cells is directly related to solar system's efficiency, therefore it dominates the photovoltaic market. However, single crystals are more effective because of expensive, cells are now often made from multicrystalline material rather than single in order to reduce costs. According to, the modules have long lifetime (20 years and more) and their best production efficiency is approaching 18% it can be said that crystalline silicon cell technology is well established. Besides, amorphous silicon solar cells are cheaper but also less efficient type of silicon cells [22].

The silicon solar cells which are made form of amorphous thin films are used to power a variety of consumer products. Larger amorphous silicon solar modules are also becoming available with the improvement in the solar industry. **Figure.I.10**. shows a new type of thin film modules are appearing on the market cadmium telluride and copper indium dieseline which is also offer low cost with acceptable conversion efficiencies. High-efficiency solar cells design from gallium arsenide, indium phosphide or their derivatives are used in specialized applications such as to power satellites or in systems which operate under high- intensity concentrated sunlight.

Figure I.10 : *Amorphous-Si solar panel [22].*

In **Figure. I.11** shows below the structure of a typical silicon solar cell. The electrical current generated in the semiconductor is extracted by contacts to the front and back of the cell. As can been seen at the top contact structure also called finger should be allow light to pass through that supply current to a larger bus bar. Transparent conducting oxide is also used on a number of thin film devices. When solar cell absorbing the sunlight meantime it should be minimize the reflection of light in order to increase the efficiency. This is called the antireflection coating (ARC) which is covered with a thin layer of dielectric material [22].

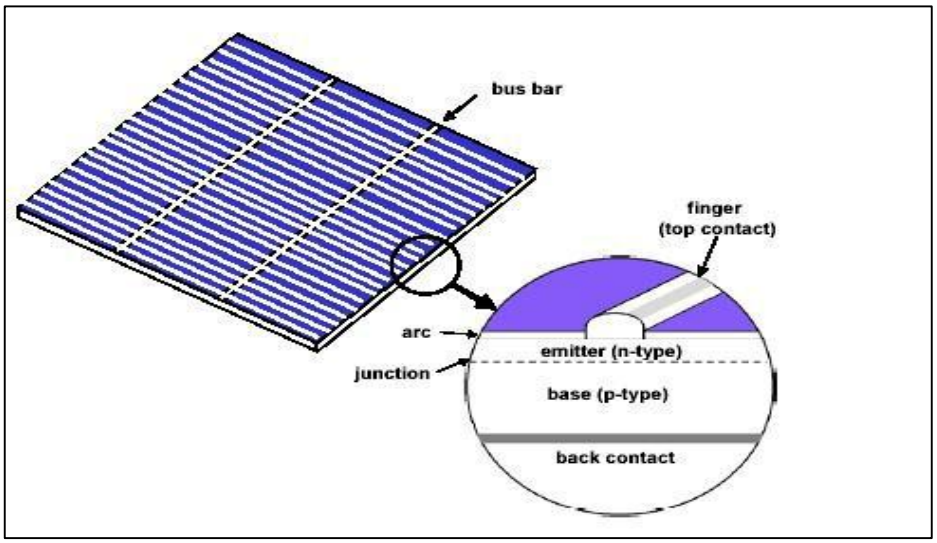

Figure I.11 : *The structure of a typical crystalline silicon solar cell [22]*

The energy transformation in solar cells is different from the classical heat engine process, so the limitations and losses that occur in more detail. The fundamental mechanisms responsible for losses in solar cells are explicit from the discussion of solar cell operation. A considerable part of the solar spectrum is not utilized because of the inability of a semiconductor to absorb the below-band gap light which causes from the heat is produced on carrier generation in the semiconductor by photons with energy in excess of the band gap. Losses can be reduced, a device called tandem cell because going over to more complex structures based on several semiconductors with different band gaps. The top cell of tandem is made of a high band gap semiconductor, and converts the short wavelength radiation. The transmitted light is then converted by the bottom cell. This adjustment tenders considerably the achievable efficiency for the system. High efficiency space cells operating at close to 30% are available [22].

Other losses reduce the efficiency of devices, 50% is the achievable at maximum, some thin-film devices it is less. Non-radiative recombination of the photo generated electron hole pairs is the common loss mechanisms which is present in all practical devices. Such recombination is most common because of pollution or impurities, and defects of the crystal structure, or at the surface of the semiconductor

where energy levels may be introduced inside the energy gap. These levels act as stepping stones for the electrons to fall back into the valence band and recombine with holes. Measures taken to minimize the recombination losses include careful processing to maintain long minority carrier lifetime, and protecting the external surfaces of the semiconductor by a layer of passivating oxide to reduce surface recombination. The contacts can be surrounded by heavily doped regions acting as "minority carrier mirrors" which impede the minority carriers from reaching the contacts and recombining. The losses to current with the rejoin are often grouped under the term of collection efficiency which is the ratio between the number of carrier generated by light and the number that reaches the junction. Considerations of the collection efficiency affect the design of the solar cell. In crystalline materials, the transport properties are usually good, and carrier transport by simple diffusion is sufficiently effective. In amorphous and polycrystalline thin films, however, electric fields are needed to pull the carriers. The junction region is then made wider to absorb the main part of the photon flux. Other losses to the current produced by the cell arise from light reflection from the top surface, shading of the cell by the top contacts, and incomplete absorption of light. The last feature can be particularly significant for crystalline silicon cells since silicon – being an indirect-gap semiconductor - has poor light absorption properties. Measures which can be taken to reduce these losses include the use of multi-layer antireflection coatings, surface texturing to form small pyramids, and making the back contact optically reflecting. When combined with a textured top surface, this geometry results in effective light trapping which provides a good countermeasure for the low absorptivity of silicon. Top-contact shading is reduced in some cells by forming these contacts in narrow laser grooves, or all the contacts can be moved to the back of the cell. Another loss in commercial cells is ohmic losses in the transmission of the current produced by the solar cell, usually grouped together as a series resistance, which reduce the fill factor of the cell. The principal characteristics of different types of cell in or near commercial production are summarizes in **table I.3** below.

Material	**Area (cm^2)**	**Best Efficiency (%)**	**Technology**
Mono or multi cryst. silicon	10	25	Plate/wafer
Amorphous silicon	5	3	Thin film
Copper indium dieseline	8	16	Thin film
Cadmium telluride	7	16	Thin film

***Table I.3** : Solar cell efficiencies achieved by the principal semiconductor technologies.[24]*

In addition, to crystalline silicon, much effort is focused on the manufacture of thin- film devices which have lower material requirements. Furthermore, there is considerable research activity in purely molecular materials and photovoltaic materials are no longer dependent onto semiconductors. A number of research groups have showed solar cells based on conducting polymers, often in combination with fullerene derivatives as electron acceptors to create the p-n junction. There is much to look forward to if their success matches the achievements of the LED technology.

Amorphous silicon is one of a number of thin film technologies. This type of solar cell can be applied as a film to low cost substrates such as glass or plastic. Other thin film technologies include thin multicrystalline silicon, copper indium dieseline/cadmium sulphide cells, cadmium telluride/cadmium sulphide cells and gallium arsenide cells. There are many advantages of thin film cells including easier deposition and assembly, the ability to be deposited on inexpensive substrates or building materials, the ease of mass production, and the high suitability to large applications [24].

I.2.3.2. Work principle of solar cells

We need to consider both the nature of the material and the nature of sunlight in order to understand the operation of a PV cell. Solar cells consist of two types of material, first often p-type silicon and secondly n-type silicon. Wavelengths of a certain light is able to ionize the atoms in the silicon and the internal field produced by the junction separates some of the positive charges (holes) from the negative charges (electrons) within the photovoltaic device. The holes are swept into the positive layer and the electrons are swept into the negative layer. Although these opposite charges are attracted to each other, because of the internal potential energy barrier most of them can only rejoin by passing through an external circuit outside the material. Therefore if a circuit is made, power can be produced from the cells with lighting, so the free electrons have to pass through the load to rejoin with the positive holes.

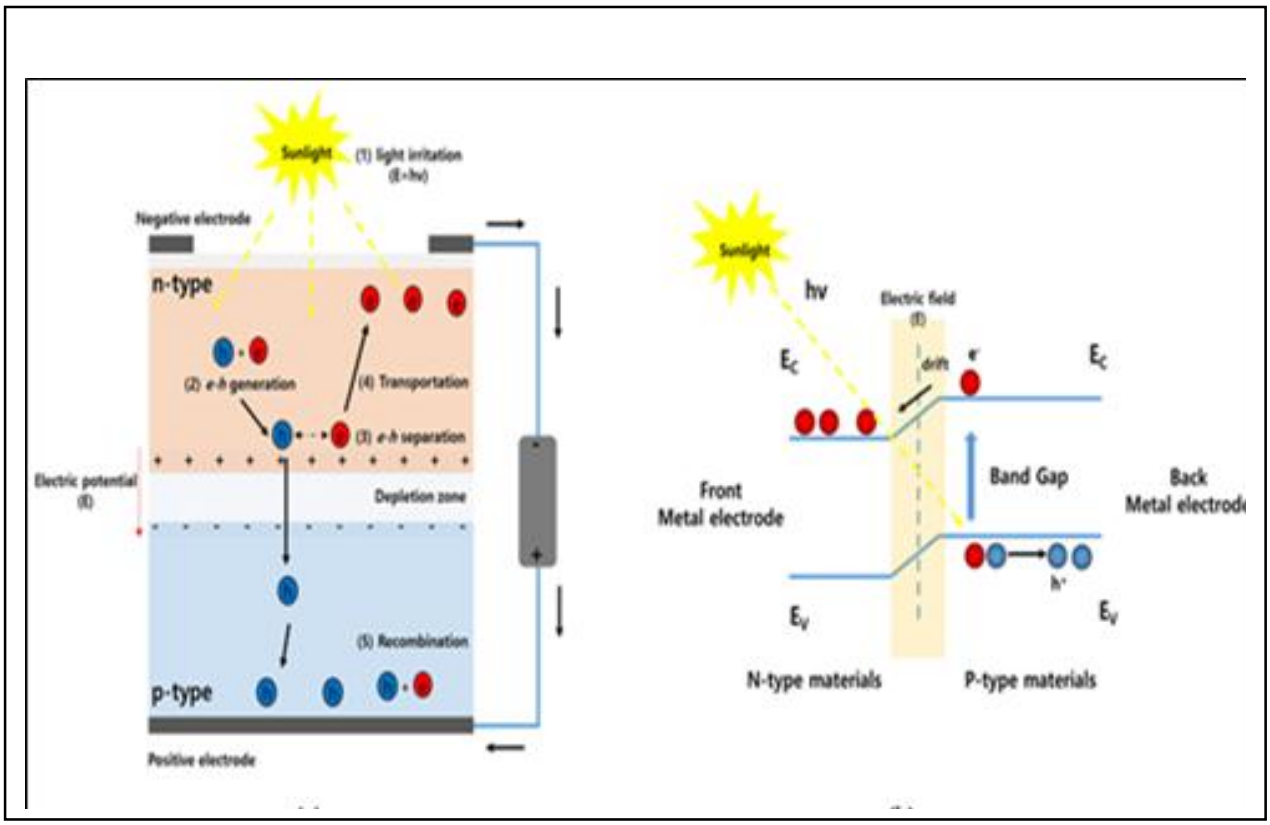

Figure I.12 : *(a) working principle of solar cell with p-n junction structure and (b) loss mechanism in standard p-n junction solar cells [25]*

The power gained from a PV device is regulated by;

- ✓ First, the type and area of the material,
- ✓ Second, the wavelength of the sunlight,
- ✓ Third the intensity of the sunlight.

Single crystal silicon solar cells can not convert more than 25% of the solar energy into electricity, because of the radiation in the infrared region of the electromagnetic spectrum does not have enough energy to separate the positive and negative charges in the material.

Because of the higher internal energy losses than a single crystal silicon, polycrystalline silicon solar cells have an efficiency of less than 20% and amorphous silicon cells are presently about 10% efficient. A typical single crystal silicon PV cell of 100 can produce about 1.5 watts of power at 0.5 volts DC and 3 amps under full sunlight (1000). The power output of the cell is directly proportional to the intensity of the sunlight. It means for example, if the intensity of the sunlight is halved the power will also be halved.

Another important feature of PV cells is that the voltage of the cell does not depend on its size, and remains fairly constant with changing light intensity. However, the current in a device is almost directly depend to light intensity and size. When we look different sized cells, we need to record the current density, or amps per square centimeter of cell area.

To increase the power output of a solar cell, it should keep the PV device directly facing the sun, or by concentrating the sunlight using lenses or mirrors. However, there are limits to this process, due to the complexity of the mechanisms, and the need to cool the cells. Temperature affects the voltage. The current output is relatively constant at higher temperatures, but the voltage is reduced, leading to a drop in power as the cell temperature is increased [26].

I.2.3.3. Types of Solar Cells

The solar cell technology is very rich corresponding to substance used and production type. There are more than dozen of substances besides lots of them are being working progress in order to produce a solar cell. Principal types of solar cells are as follows [27]. Solar cells can be categorized in three parts.

- First Generation Solar Cells (Crystalline Silicium).
- Second Generation Solar Cells (Thin Film).
- Third Generation Solar Cells (Nanotechnology based solar cells).

I.2.3.3.1. First Generation Solar Cells

The first generation of solar cells, developed in the 1950s and 1960s, primarily used crystalline silicon as the semiconductor material. These cells were notable for their initial efficiency improvements and paved the way for modern photovoltaic technology. However, their manufacturing costs remained high, limiting widespread adoption until further advancements were made.

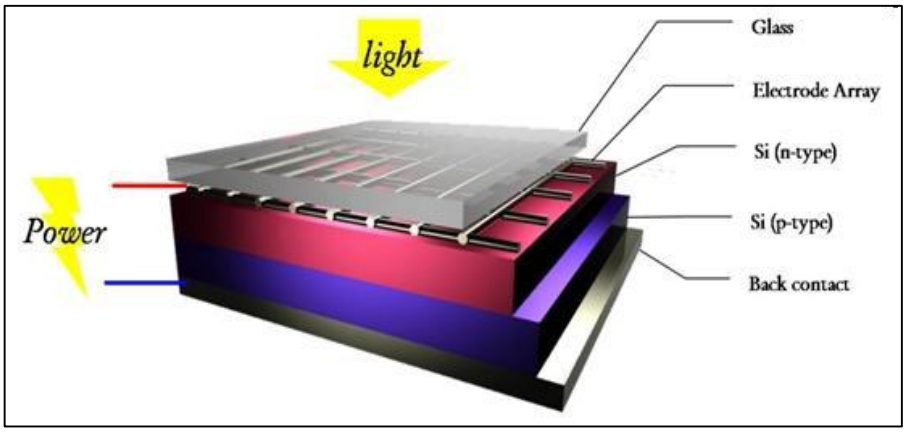

Figure I.13 :*First Generation Solar Cell [23]*

I.2.3.3.2. Second Generation Solar Cells

The second generation of solar cells, emerging in the 1980s, introduced thin-film technologies such as amorphous silicon, cadmium telluride, and copper indium gallium selenide (CIGS). These cells aimed to reduce costs through cheaper materials and flexible substrates, offering improved efficiency and opening new applications in building-integrated photovoltaics and portable electronics.

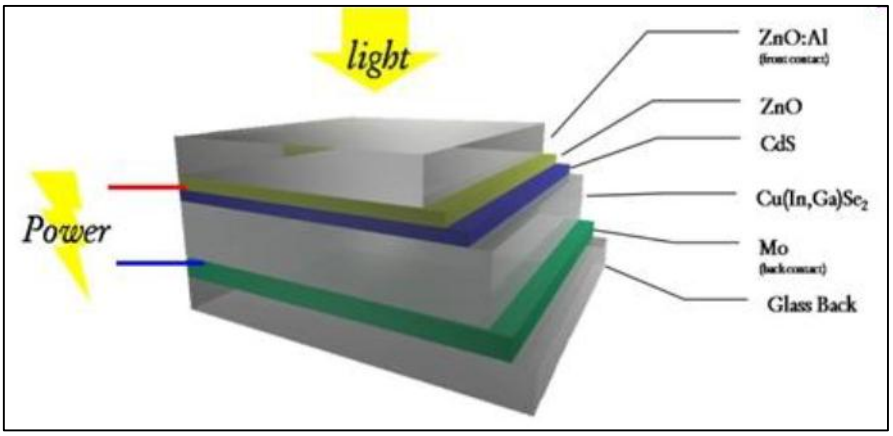

Figure I.14 : *Second Generation Solar Cell [23]*

a. Thin Film Solar Cells

In this technic, aim is the reduce thickness of the cell with using substances which has higher quality to absorb light. Absorption coefficient of amorphous silicium solar cells is greater than crystalline type solar cells' coefficient. For example, even 1 micron thick amorphous silicium can absorb the light radiation in a region with wavelength is 0.7, to absorb the same light crystal silicium has to be at 500 microns thick. Therefore, amorphous silicium has advantage because using less material for made [23].

b. Amorphous Silicium Solar Cells

Amorphous silicium solar cells are the primary sample of thin film technology of solar cells. However, first made (a-Si) solar cells are in Schottky barrier structure, then p-i-n junction structures are developed. Laboratory efficiency is about 27% but the real efficiency is between 8 and 10%. High costs materials are needed during fabric phase but sometimes firms prefer this type because of production duration is cheap [23].

c. Copper Indium Diselenoide Solar Cells

This type of solar cells consists of coming together elements in first, third and sixth groups of periodic table. Its absorption coefficient is very high. This compound (CIS) is made of from copper, indium, and selenium are called as CIS solar cells. With the contribution of the gallium in the compound obtained greater efficiency. However, as increase in the number of elements in the compound makes situation complex to control properties or contributions of elements for the system. For small area laboratory cell efficiency is about 20% but 1m² solar module efficiency is about 16%. There are two methods in production, first vaporizing the elements in a vacuum simultaneously. Second, reacting the copper indium thin film alloy with selenium in a suitable environment which is also called selenization. In both cases, purpose is to establish a diode between the plates [23].

d. Cadmium Telluride Solar Cells

This type of solar cells is made with simple methods and they are cheap. It has the shortest energy payback time of all solar technologies. However, experimental efficiency is up to 17%, for 8m² solar module's efficiency is about 9-10%.

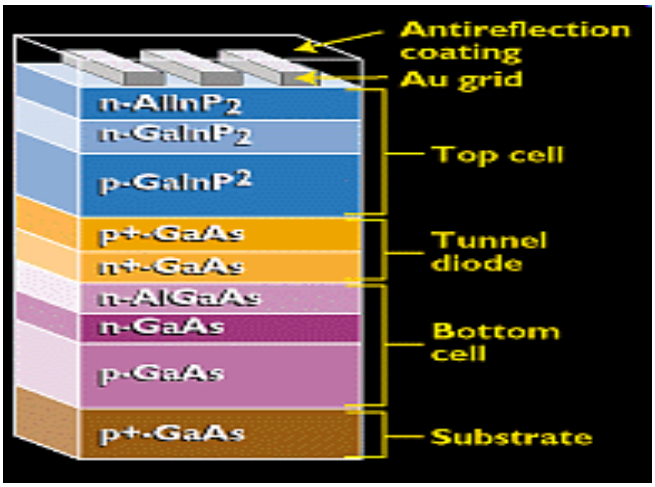

Figure I.15 :*Schematic display of third generation solar cells [23]*

I.2.3.3.3. Third Generation Solar Cells

Third generation or as known as multi-junction solar cells enhance poor electrical performance while maintaining very low production costs. Current researches are targeting conversion efficiencies of 30% - 60% while retaining low cost materials and manufacturing techniques. However, these researches are still ongoing for this technology and there are no solid conclusions so far. It will be big progress about energy subject if they are in fabric because they submit super high value efficiency comparing to present ones [23].

Reference

[1] A.W.M.; Abdullah, S.F.; Chau, C.F.; Ghazali, A.; Ahmad, I.; Abdullah, W.S.W. Effect of Chemical Bath Deposition Variables on the Properties of Zinc Sulfide Thin Films: A Review. Academic Editor: Federico Bella, Published: 20 March 2023

Molecules 2023, 28, 2780. doi.org/10.3390

[2] Wells, A. F., Structural Inorganic Chemistry (5th ed.), Oxford: Clarendon Press, 1984, ISBN 0-19-855370-6.

[3] Fang X., Zhai T., Gautam U.K., Li L., Wu L., Bando Y., Golberg D., ZnS nanostructures: From synthesis to applications, Prog. Mater. Sci., Vol. 56(2), 2011.

[4] Biswas S., Kar S., Fabrication of ZnS nanop333articles and nanorods with cubic and hexagonal crystal structures: a simple solvothermal approach, Nanotechnology, Vol. 19(4), 2008.

[5] Chen H., Shi D., Qi J., Jia J., Wang B., The stability and electronic properties of wurtzite and zinc-blende ZnS nanowires, Phys. Lett. A, 373,(3), 2009, 371–375.

[6] Fan L., Song H., Zhao H., Pan G., Yu H., Bai X., Li S., Lei Y., Dai Q., Qin R., Wang T., Dong B., Zheng Z., Ren X., Solvothermal synthesis and photoluminescent properties of ZnS/cyclohexylamine: inorganic-organic hybrid semiconductor nanowires, J. Phys. Chem. B, Vol. 110(26), 2006, 12948–12953.

[7] A.A. Ibiyemi, A.O. Awodugba, «The Influence of Annealing on Electrical and Optical Properties of ZnS Thin Film,» *The Pacific Journal of Science and Technology*, vol. 13(1), pp. 213-220, 2012.

[8] Rohwer L.S., Nalwa H.S., Handbook of Luminescence, Display Materials, and Devices: Display devices, American Scientific Publishers, 2003.

[9] Chen H., Shi D., Qi J., Jia J., Wang B., The stability and electronic properties of wurtzite

and zinc- blende ZnS nanowires, Phys. Lett. A, Vol. 373,(3), 2009, 371–375.

[10] Bryan J.D., Gamelin D.R., Doped Semiconductor Nanocrystals: Synthesis, Characterization, Physical Properties and Applications, Prog. Inorg. Chem., Vol. 54, 2005, 47–126.

[11] Zhao Y., Hong J.M., Zhu J.J., Microwave-assisted self-assembled ZnS nanoballs, J. Cryst. Growth, Vol. 270(3–4), 2004, 438–445.

[12] Tesla, Nikola "The Inventions, Researches, and Writings of Nikola Tesla", 1894, Internet Archive. p. 290. Retrieved 2 January 2024.

[13] Franz, K. A., Kehr, W. G., Siggel, A., Wieczoreck, J., & Adam, W. (2000). *Luminescent Materials. Ullmann's Encyclopedia of Industrial Chemistry.* doi:10.1002/14356007.a15_519.

[14] Wang, Gang; Huang, Baibiao; Li, Zhujie; Lou, Zaizhu; Wang, Zeyan; Dai, Ying; Whangbo, Myung-Hwan, Synthesis and characterization of ZnS with controlled amount of vacancies for photocatalytic H2, production unde visible light, Scientific Report, 2015.doi :10.1038.

[15] Bruinguier E ,tentative anatomy of ZnS-type electroluminescence, J. Appl. Phys, Vol. 75(9), 1994, 4291-4321.

[16] Siju Mishra, D. Haranath, **Nanoscale Compound Semiconductors and their Optoelectronics Applications** , Woodhead Publishing Series in Electronic and Optical Materials. 2022, Pages 47-66.

[17] G. N. Tiwari, Solar Energy: Fundamentals, Design, Modelling and Applications, Narosa, Publishing House, New Delhi, India, 2004.

[18] A. Hamache, Study of the type inversion of the semiconductor in irradiated solar cells, doctorat thesis, Mohamed Khider University, 2018.

[19] A. Ghania, STUDY OF SILICON SOLAR CELLS PERFORMANCES USINS THE IMPURITY PHOTOVOLTAIC EFFECT ? DOCTORAT thesis, Université Ferhat Abbas-Setif, 2012.

[20] M. A. Green, Solar cells, Operating Principles Technology, and Systems, Prentice-Hall, 1982.

[21] P. Nwofe, *Deposition and Characterisation of SnS Thin Films for Application inPhotovoltaic Solar Cell Devices, PhD thesis, University of Northumbria at Newcastle,* 2013.

[22] Ç.Şule, Photovoltaic power generation for polycrystalline solar cells and turning sunlight into electricity, U.G., Engineering Physics, Thesis, Gaziantep, (2005).

[23] Tunahan Işık, Solar Cells Review, Thesis, Işık university,January-2015.

[24] R., Messenger, J.Ventre, Photovoltaic systems engineering. Boca Raton, FL: CRC Press, 348, (2000).

[25] Kim, S.; Hoang, V.Q.; Bark, C.W. Silicon-Based Technologies for Flexible Photovoltaic (PV) Devices: From Basic Mechanism to Manufacturing Technologies. Nanomaterials 2021, 11, 2944gies. Nanomaterials 2021, doi.org/10.33903/nano11112944.

[26] Martin A.Green, Keith Emery, Yoshihiro Hishikawa, Wilhelm Warta, Ewan D.Dunlop, rogress in photovoltaics, researche and Applications, published IWiley online library, vol.23,2015.doit10.1002/pip.2573.

[32] B.Godfrey, Renewable Energy Power for a Sustainable Future,the open university of oxford, 78, (2004).

Chapter II :elaboration & characterization techniques

In this chapter, we will discuss several techniques applied to the study of zinc sulfide, each playing a crucial role in determining its distinct properties. To assess optical properties, we employ spectrophotometry, while the Hall effect technique is utilized for electrical properties. Additionally, X-ray diffraction is employed to analyze structural properties. Furthermore, we will explore the use of ultrasonic spray technique in the fabrication of thin films.

II.1 Hall Effect Technique

II.1.1. Introduction

It was in 1879 that E.H. Hall1 from Harvard University reported the results of an experiment which had enabled him to determine the sign of a driver's load-bearers. The figure below illustrates the principle of Hall's experiment [1].

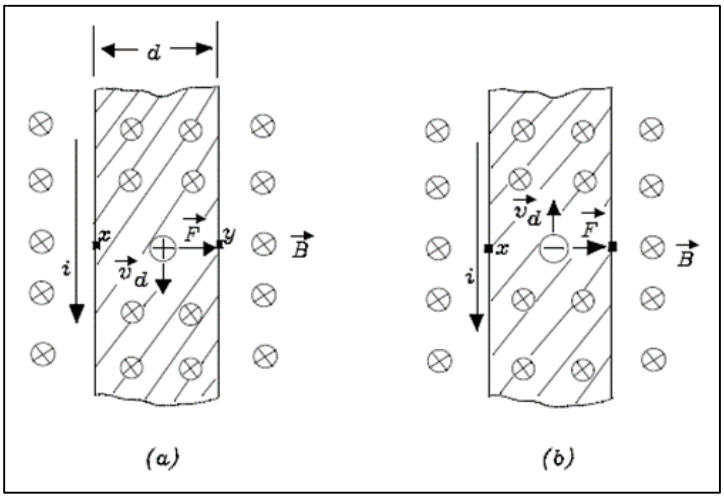

Figure II.1 : *The principle of Hall's experiment [1].*

A conductive tape is placed in a magnetic induction field $\vec{B}$ perpendicular to the plane from the sheet. The field gives rise to the appearance of a deflection force $\overrightarrow{F}$ who acts towards the right, it does not matter if the charge carriers are positiveor negative. It then appears a voltage Vxy called Hall voltage, the sign of which makes it possible to determine the type of the carriers of loads. If the carriers are positive (a), the potential at y is higher than that at x; if the carriers are negative (b), the potential at y is lower than that at x. Experience demonstrates that in most metals the charge carriers are negative.

II.1.2. Working principale

The Hall effect technique is based on a fundamental principle of physics known as the Hall effect. Here's a simplified explanation of its working principle:

a. Electric Field Application : A sample material, typically a semiconductor or metal, is placed in a magnetic field created perpendicular to the direction of current flow through the material.

b. Lorentz Force : When a current flows through the material in the presence of a magnetic field, each moving charge carrier (electron or hole) experiences a Lorentz force perpendicular to both the direction of the current and the magnetic field.

c. Hall Voltage : The Lorentz force causes a charge separation within the material, creating an electric field perpendicular to both the current and the magnetic field. This results in a measurable voltage across the sample, known as the Hall voltage (V-H).

d. Measurement : The Hall voltage (V-H) is proportional to the product of the magnetic field strength (B), the current (I) flowing through the material, and a characteristic parameter known as the Hall coefficient (R-H) of the material:

$$V_H = R_H \frac{I.B}{t} \qquad (1)$$

Where:

R_H is the Hall coefficient; **I** is the current flowing through the material; **B** is the magnetic field strength and **t** is the thickness of the material (in the direction perpendicular to the current flow and magnetic field).

e. Analysis : By measuring the Hall voltage (V-H), one can determine the sign (whether the charge carriers are electrons or holes) and density of the charge carriers in the material, as well as the mobility of the charge carriers.

In summary, the Hall effect technique utilizes the generation of a Hall voltage due to the interaction of moving charge carriers with a magnetic field to study the type, concentration, and mobility of charge carriers in semiconductors and metals.

II.1.3. Principle of measurement

A constant current is circulated inside the sample using a current source (see the specifications of the source). The resistivity voltage, the Hall voltage and the analog output of the gaussmeter are sent to channels 1, 2 and 3 of the scanner. The temperature is first stabilized by using the temperature controller, then the voltages present at the terminals of the three channels are measured using the multimeter. These same measurements are carried out in the presence of the magnetic field (in both polarities) as well as in its absence. It is the field inverter that makes it possible to switch from one polarity to the other without having to manually disconnect the current leads of the electromagnet [4].

II.2. X-Rays Diffraction Technique

II.2.1. Introduction

X-rays were discovered in 1895 by the German physicist armentgen and are the basis of various techniques From analyzes such as radiography, spectroscopy and diffraction measurement. These electromagnetic radiations haveThe wavelength of the order of the ochngster ochnum (1 = = 10-10 m). A crystal is an arrangement of atoms, ions or molecules, with a pattern that repeats periodically in The three dimensions. The distances between atoms are of the order of auchengster-auchemmen, of the same order of magnitude as X-ray wavelengths: the crystal therefore forms a 3D network capable of neutralizing X-rays. In 1913, William Lawrence Bragg and his father Sir William Henry Bragg used this radiation to determine The crystalline structure of sodium chloride and then many other mineral salts. Together they received the award Nobel Prize in physics in 1915 for his contributions to "the analysis of the crystal structure by X-ray". We present the basic theory of the interaction of X-rays with solid structures as well as the implementation Examples of applications: the precision of the crystal structure on single crystals and the recognition of Phases in crystalline solids [8].

II.2.2. Definition of X-Rays diffraction

X-rays is generally carried out according to the same process as that used in medical imaging.Electrons torn from an electrically heated tungsten filament are accelerated under the effect of a field intense electrical (voltage of 50 kV) to bombard an anode (or anticathode) made of different materials depending on the intended applications. The X-rays are emitted by the anode according to two mechanisms [8].

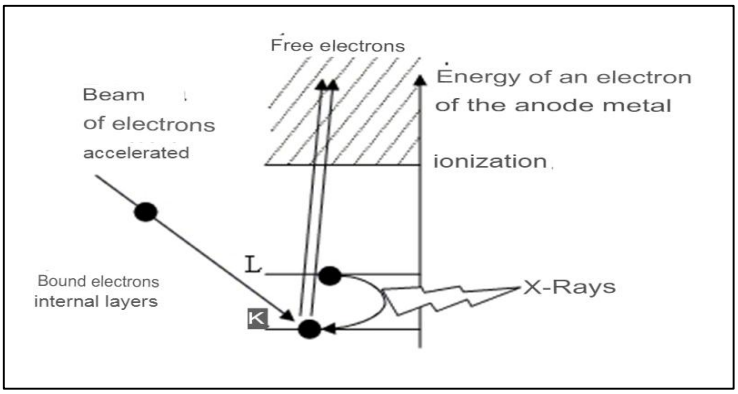

Figure II.2: *Electronic transitions responsible for theproduction of X-rays [8]*

The two metals commonly used for the anode are copper, which produces wavelength X-rays; λ = 1.54 Å and molybdenum λ = 0.709 Å. To have an optimal diffraction, it is necessary use a wavelength radiation of the same order of magnitude as the size of the network, here the space interatomatic. This is why molybdenum-based sources are suitable for structural resolution on single crystal of small molecules. Copper is used in the case of macromolecules (as a protein) and for powder analyses because it allows a better separation of diffraction spots. Another source of X-ray radiation is the synchrotron. Indeed, any charged particle in motion emits a continuous electromagnetic radiation (synchrotron radiation) covering a wide frequency range from the far ultraviolet to the X-ray. The intensity of synchrotron radiation greatly exceeds that of other sources. The use of such an instrument is reserved for the most difficult cases, to highlight details very fine or to characterize crystals with very small dimensions (of the order of ten micrometers) [8].

II.2.3. working Principle

This characterization method makes it possible to highlight information on the crystal structure of the materials (for example their texture and their degree of crystallinity) [5]. The diffraction phenomenon results from the interaction of an electromagnetic wave, such as X-rays, with the periodic medium of the crystallized material. X-ray diffraction of pulverulent samples (called "X-ray diffraction on powder") is commonly used for the characterization of solids. The term powder simply means that the incident X-ray beam is sent to a set of randomly oriented crystallites, sufficiently numerous for all the orientations to be achieved [5].

When a parallel monochromatic X-ray beam of wavelength λ (between 0.1 A° (hard X-rays) and 50 A° (soft X-rays)) is radiated onto a crystalline material with an angle of incidence, the reticular atomic planes (hkl) of the crystal, equidistant from dhkl (inter-reticular distances), will behave like parallel

mirrors and reflect the electromagnetic wave, inducing a diffraction phenomenon. The diffracted intensity will be non-zero only if the contributions of the successive planes are in phase (constructive interferences), that is to say if Bragg's law is respected (1)

$$2d_{hkl}.\sin\theta = n\,\lambda \qquad (2)$$

λ is the wavelength of the X-ray beam; d_{hkl} is the inter-reticular distance; θ: Incidence angle of the X-rays and n is the order of diffraction.

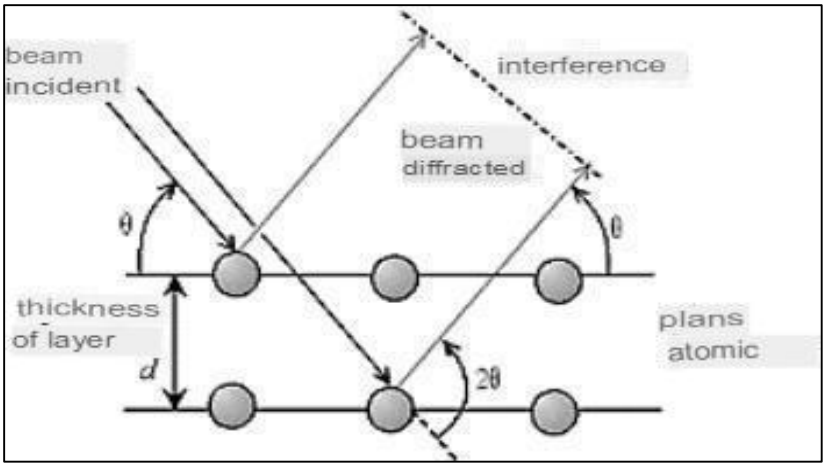

Figure.II.3: *Principle of Bragg's law [6]*

When the angle of incidence corresponds to a Bragg angle for the fixed wavelength, a diffraction peak is recorded, the intensity of which is measured. The powder method provides a list of the couples (θ, I) and, the wavelength being known, the angle can be directly converted into the inter-reticular distance (2) :

$$2d_{hkl} = n\lambda / \sin\theta \qquad (3)$$

Fig.II.8. presents the diagram of the most common principle, which is a so-called Bragg-Brentano reflection assembly. The incident radiation is monochromatic. The source S is linear and perpendicular to the plane of incidence. It is placed on the circle(C) of the diffractometer. The sample (E) is such that its reference plane passes through the axis of the diffractometer C and rotates around this axis with an adjustable speed ω. The window F of the counter also moves on the circle (C), at a double angular velocity 2ω. For an angle of zero incidences, S, F and C are aligned. A scanning (θ, 2θ) is thus carried out [8].

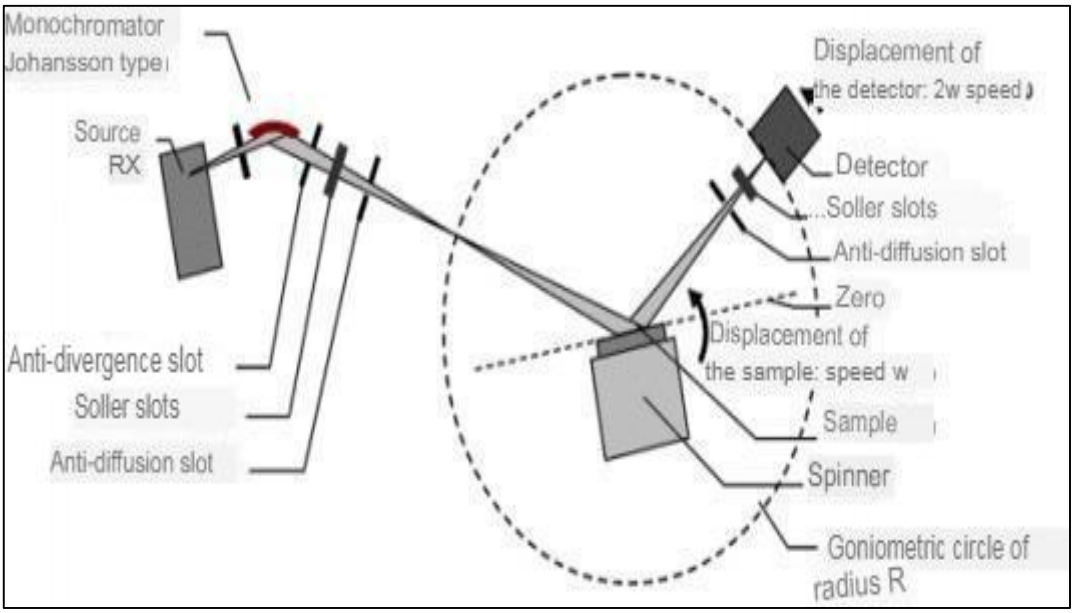

Figure.II.4: *Principle of the diffractometer in Bragg-Brentano geometry [7]*

The X-ray diffractogram (diffraction pattern) is obtained from the data collected by a detector. For each crystalline sample, the constructive interferences are observed in the form of "diffraction peaks". A given crystalline phase generates diffraction peaks always in the same directions, constituting a true signature that allows its identification. The diffraction peaks can then be identified by comparing with the sheets of the compounds referenced in the database, in the form of PDF - Powder Diffraction File (formerly JCPDS (JoinCommittee for Powder Diffraction Standards). These sheets list, for each phase, the inter-reticular distance (calculated from position 2θ by Bragg's law) and the relative intensity of each peak with respect to the most intense peak [8].

II.2.3.1 Bragg's law

A crystal can be seen as the three-dimensional periodic repetition of elements (atoms or molecules), called nodes, identified by black disks in Fig.II.9. The diagram represents a section of planes reticulars passing through the centers of these elements, spaced apart by a distance d. The angle θ (Bragg angle) determines the incidence of a parallel beam of X-rays on these reticular planes. Note that θ is the complementary to the usual angle of incidence in optics. The optical path difference between the two rays the particulars represented is equal to AC + CB = 2 d sinθ. They interfere in a constructive way when the .path difference is equal to an integer p of wavelength. This is Bragg's law [8].

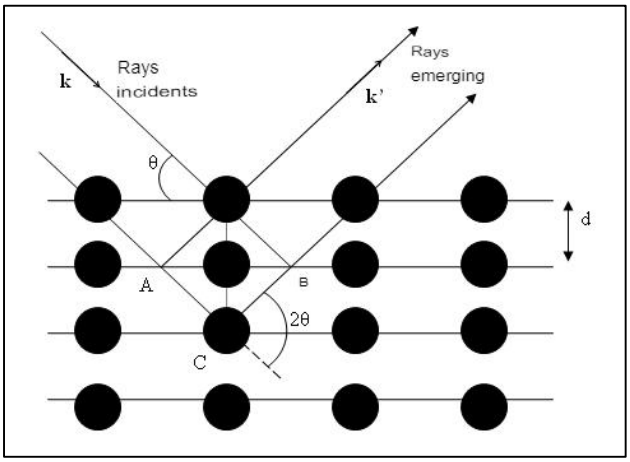

Figure II.5: *Reflection of X-rays by a family of reticular planes spaced apart by a distance d [8]*

II.2.3.2. Analysis of the intensity of the diffraction spots

The intensity of the diffracted light signal is important to analyze. Indeed, it depends on the nature of the atoms and of their positions according to the structure factor: with xj , yj , zj , the coordinates of the atom j in the mesh, fj(sinθ/λ), the form factor of the atom j and Bj the factor of thermal agitation. The latter reduces the diffraction coherence between equivalent atoms in meshes different. The factor fj(sinθ/λ) varies as a function of the Bragg angle θ; it is equal to the atomic number Z of the atom when the X-ray beam is not deflected (θ = 0), because the entire electronic procession of the atom participates in diffraction. When θ increases, it decreases, due to the loss of coherence between the scattered waves by different portions of the atom. For each chemical element, the variation of the function f(sinθ/λ) is modeled by a superposition of four exponentials : whose parameters ai, bi and c are tabulated.

The measured intensity is proportional to the square of the modulus of the structure factor and makes it possible to determine the atomic nature of the chemical elements and their position in the mesh; it is therefore possible to characterize entirely the crystalline pattern.

II.3. Spectrophotometry technique

II.3.1. Introduction

Spectrophotometry is a branch of electromagnetic spectroscopy that is concerned with the quantitative measurement of the reflection or transmission properties of matter as a function of wavelength.[9] spectrophotometry uses photometers, known as spectrophotometers, which can measure the intensity of a light beam at different wavelengths. Although spectrophotometry is most commonly applied to ultraviolet, visible, and infrared radiation, modern spectrophotometers can interrogate large

areas of the electromagnetic spectrum, including X-ray, ultraviolet, visible, infrared, and/or microwave waves.

II.3.2. Definition

Spectrophotometry is a tool that hinges on the quantitative analysis of molecules depending on how much light is absorbed by colored compounds. Important features of spectrophotometers are spectral bandwidth (the range of colors it can transmit through the test sample), the percentage of sample transmission, the logarithmic range of sample absorption, and sometimes a percentage of reflectance measurement [10].

II.3.3. Working principle

A spectrophotometer is commonly used for the measurement of transmittance or reflectance of solutions, transparent or opaque solids, such as polished glass, or gases. Although many biochemicals are colored, as in, they absorb visible light and therefore can be measured by colorimetric procedures, even colorless biochemicals can often be converted to colored compounds suitable for chromogenic color-forming reactions to yield compounds suitable for colorimetric analysis [10]. However, they can also be designed to measure the diffusivity on any of the listed light ranges that usually cover around 200–2500 nm using different controls and calibrations.[9] Within these ranges of light, calibrations are needed on the machine using standards that vary in type depending on the wavelength of the photometric determination [11].

The absorption of light is due to the interaction of light with the electronic and vibrational modes of molecules. Each type of molecule has an individual set of energy levels associated with the makeup of its chemical bonds and nuclei and thus will absorb light of specific wavelengths, or energies, resulting in unique spectral properties [12]. This is based upon its specific and distinct makeup.

II.3.4. Uses of spectrophotometers

- The use of spectrophotometers spans various scientific fields, such as physics, materials science, chemistry, biochemistry, chemical engineering, and molecular biology [13].
- They are widely used in many industries including semiconductors, laser and optical manufacturing, printing and forensic examination, as well as in laboratories for the study of chemical substances.

- Spectrophotometry is often used in measurements of enzyme activities, determinations of protein concentrations, determinations of enzymatic kinetic constants, and measurements of ligand binding reactions Ultimately [10].
- a spectrophotometer is able to determine, depending on the control or calibration, what substances are present in a target and exactly how much through calculations of observed wavelengths.
- In astronomy, the term spectrophotometry refers to the measurement of the spectrum of a celestial object in which the flux scale of the spectrum is calibrated as a function of wavelength, usually by comparison with an observation of a spectrophotometric standard star, and corrected for the absorption of light by the Earth's atmosphere [14].

II.3.5. Design of Spectrophotometers

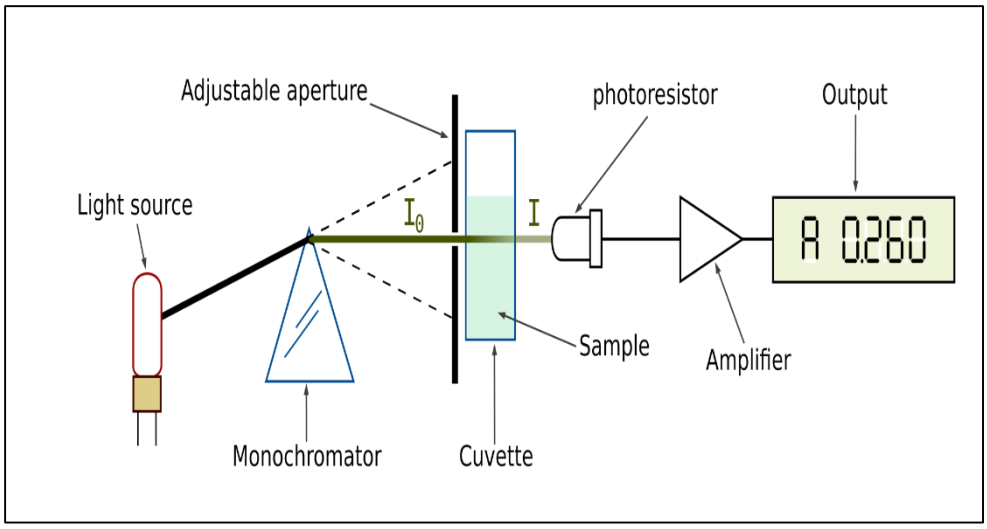

***Figure II.6** : Single-beam scanning spectrophotometer [14]*

There are two major classes of devices: single-beam and double-beam. A double-beam spectrophotometer compares the light intensity between two light paths, one path containing a reference sample and the other the test sample. A single-beam spectrophotometer measures the relative light intensity of the beam before and after a test sample is inserted. Although comparison measurements from double-beam instruments are easier and more stable, single-beam instruments can have a larger dynamic range and are optically simpler and more compact. Additionally, some specialized instruments, such as spectrophotometers built onto microscopes or telescopes, are single-beam instruments due to practicality [15].

II.4. Ultrasonic spray pyrolysis

II.4.1. Introduction

Ultrasonic Spray Pyrolysis (USP) is a simple aerosol synthetic technique widely used for the synthesis of nano-materials such as thin films or nanoparticles. Due to its easy feasibility, flexibility and cost-efficiency, the USP method is an important alternative to the chemical vapor deposition (CVD). The precursors for ultrasonic spray pyrolysis are often prepared via sol-gel route. The composition of the synthesized nano-particles or the film can be easily modified via changes of the processing parameters. Ultrasonic spray pyrolysis gives you full control over the most important process parameters such as: ultrasonic amplitude precursor solution precursor composition/ viscosity flow rate deposition temperature substrate temperature This makes the ultrasonic spray pyrolysis an interesting technology to manufacture dense and porous particles and thin-film coatings [24, 25].

II.4.2. Definition of ultrasonic spray pyrolysis

The ultrasonic spray pyrolysis (USP) technique is the droplet generation phenomenon induced by ultrasonic waves with several interesting properties including its simplicity, cost-effectivity, continuous operation, high deposition rate, and ability to deposit on broad surface areas. The size of the obtained droplets is less than 20 μm in average for low in-flight speed. This can impede the removing of droplets from the gas phase due to their collision with the reactor walls, collisions between the droplets themselves, and the consequent merging [16]. The spray pyrolysis technique has several advantages including the higher stability of the obtained coatings as compared to coatings deposited in vacuum, the diversity of its solution precursors, its cost-effectivity, and its facility.

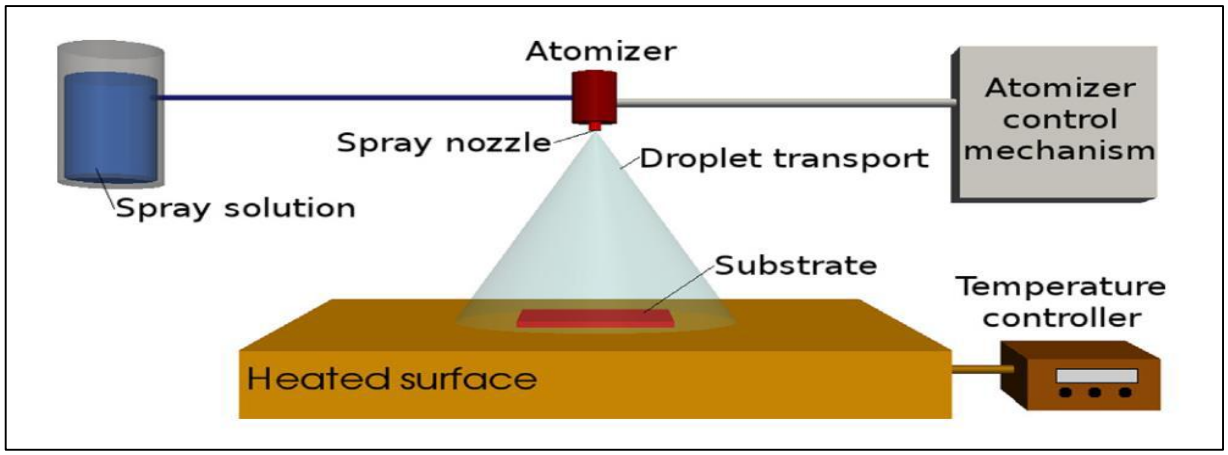

Figure II.7: *General schematic of a spray pyrolysis deposition process [23].*

I.4.3 Techniques of Spray Pyrolysis

The spray pyrolysis technique is an adaptable processing method for preparing single- and multi-layered films as dense or porous, ceramic coatings, and various material powders [17]. The existing spray processing techniques can be classified either based on the type of the energy source for the starting solution reaction for the spray pyrolysis process including tubular reactors (SP), the emulsion combustion method, vapor flame reactors, and the flame spray pyrolysis, or based on the method used for atomizing precursors, including electrostatic, air-pressurized, and ultrasonic spray pyrolysis techniques [18,19]. If the energy source used for the solution precursor reaction were from external energy supplies and not from the spray itself (as in VFSP and SP) the method would have a lower sensitivity to the precursors and solvents that have been chosen. Depending on the solubility, the type, and the cost-effectivity of solution precursors, various kinds of solvents are utilized in the spray pyrolysis technique. Typically, nitrates, chlorides, and acetates, which can be dissolved in aqueous and alcoholic solvents, are used as metal-oxide precursors [18]. Another classification of spray pyrolysis techniques is based on the type of atomizers employed in the system. Furthermore, the aerosol droplet size, which specifies the obtained film quality, depends commonly on the atomization method. There are three main atomization methods: electrostatic, air blast, and ultrasonic. The spray pyrolysis techniques that employ electrostatic, air blast, and ultrasonic atomizers are called the electrostatic spray deposition, the pressurized spray pyrolysis, and the ultrasonic or normal spray pyrolysis (SP), respectively [20]. The ultrasonic atomization operates based on an electromechanical device vibrating at high frequencies. Only Newtonian fluids with low viscosities can be atomized when being passed over the vibrating surface and the vibration causes the solution to be atomized into droplets [21].

I.4.4. Principle

The deposition technique known as "spray ultrasonic" involves the application of a fine mist or spray of material onto a substrate using ultrasonic vibrations. This technique operates on the principle of ultrasonic atomization and deposition. Here’s how it works:

a. Atomization : A liquid containing the material to be deposited is pumped through a nozzle or emitter.

b. Ultrasonic Vibration : Ultrasonic vibrations (typically in the range of 20-100 kHz) are applied to the nozzle or emitter.

c. Spray Formation : These vibrations cause the liquid at the nozzle tip to atomize into a fine mist or spray of droplets.

d. Deposition : The spray of droplets is directed onto a substrate, where the droplets coalesce and form a thin film as the solvent evaporates or is removed.

II.4.4.1. Key Features :

- ***Uniform Coating :*** Ultrasonic atomization produces a fine, uniform spray, resulting in even deposition of the material.
- ***Low Temperature Process :*** It is often used for materials sensitive to heat since it operates at relatively low temperatures.
- ***Versatility :*** Can be used for a variety of materials including metals, ceramics, and polymers, depending on the formulation of the solution/suspension.

II.4.5. Adventage of spray pyrolysis technique

As compared to the other techniques for depositing thin films, the spray pyrolysis technique has several advantages including its open-atmosphere process, its open-reaction chamber, its adjustability during the deposition, and its accessibility for observing the deposition procedure. It has also the capability of the multi-layer preparation that is very appealing for fabricating functionally graded layers. The film composition could be adjusted by varying the starting solutions. The spray pyrolysis technique is utilizable for processing dense and porous films through optimizing the deposition variables including the deposition temperature, the precursor composition and concentration, the substrate temperature, the solvent type, the carrier gas ratio, the solution flow rate, the distance existing between the setup's nozzle and substrate, and the flow rate. One major advantage of the spray pyrolysis technique as compared to vapor-phase routes is its capability in synthesizing multicomponent particles that have an exactly desired stoichiometry. Depending on the precursor type, the substrate temperature, the distance between the setup's nozzle and substrate, the droplets could be either deposited without being evaporated or completely decomposed before they can reach the substrate, which results in a process similar to the chemical vapor deposition Burning a flammable precursor may also result in the formation of a particulate spray or the enhancement of the deposition temperature [22].

II.4.5.1. Applications

- **Thin Films :** Used in the production of thin films for electronic devices, coatings, and sensors.
- **Functional Coatings :** Applied in the creation of functional surfaces with specific properties like anti-corrosion or biocompatibility.
- **Research and Development :** Commonly used in research settings due to its precise control over film thickness and composition.

Reference

[1] Rowland's Physics. Physics Today, juillet 1976.

[2] Proceedings of Physical Society A (1952), 65, 903.

[3] c.f. R.A. Smith dans Semiconductors. Cambridge University Press, 1959 p. 118. (Qc611.S45)

[4] Guy Bernier, coordonnateur des travaux pratiques Département de Physique, U. de Sherbrooke

[5] K. J. Murata, M. B. Norman, American Journal of Science, vol. 276, pp. 112- 1130, 1976.

[6] [En ligne]. Available: http://urlz.fr/1UPj. [Accès le 06 05 2015].

[7] N. Gascoin, P. Gillard, G. Baudry, Characterisation of Oxidised Aluminium Powder: Validation of a new Anodic Oxidation Bench, J. Hazard. Mater, vol. 171, pp. 348- 357, 2009.

[8] Christophe Aronica, Erwann Jeanneau, DIFFRACTION DES RAYONS X TECHNIQUES ET ÉTUDES DES STRUCTURES CRISTALLINES, Publié par Catherine Simand, culture science phyzique,vol(10). 28/10/2009

[9] Allen, DW; Cooksey, C; Tsai, BK (Nov 13, 2009). "Spectrophotometry". NIST. Retrieved Dec 23, 2018.

[10] Ninfa AJ, Ballou DP, Benore M (2010). Fundamental Laboratory Approaches for Biochemistry and Biotechnology (2nd ed.). Hoboken: Wiley & Sons. ISBN 9780470087664. OCLC 488246403.

[11] chwedt G (1997). The essential guide to analytical chemistry. Translated by Brooks H. Chichester, NY: Wiley. pp. 16–17. ISBN 9780471974123. OCLC 36543293.

[12] Ninfa AJ, Ballou DP (2004). Fundamental laboratory approaches for biochemistry and biotechnology. Hoboken: Wiley. p. 66. ISBN 9781891786006. OCLC 633862582.

[13] Rendina G (1976). Experimental Methods in Modern Biochemistry. Philadelphia, PA: W. B. Saunders Company. pp. 46-55. ISBN 0721675506. OCLC 147990.

[14] Oke, J. B.; Gunn, J. E. (1983). "Secondary standard stars for absolute spectrophotometry". The Astrophysical Journal. 266: 713. Bibcode:1983ApJ...266..713O. doi:10.1086/160817.

[15] "Fully Automatic Double Beam - Atomic Absorption Spectrophotometer (AA 8000)". Laboratory Equipment. Labindia Analytical Instruments Pvt. Ltd. Archived from the original on 2018-12-02. Retrieved 2018-01-31

[16] D. Beckel et al. J. Power Sources(2007)

[17] S. Gürmen et al. Mater. Res. Bull.(2006)

[18] S.E. Pratsinis Prog. Energy Combust. Sci. (1998)

[19] W. Daranfed et al. J. Alloys. Compd. (2012)

[20] G.S. Lonakar et al. Org. Electron. (2012)

[21] S.-Y. Park et al. Sol. Energy Mater. Sol. Cells (2011)

[22] J.-S. Kim et al. Sens. Actuators B Chem. (2016)

[23] Lado Filipovic, Siegfried Selberherr, Giorgio C. Mutinati, Elise Brunet, Stephan Steinhauer, Anton Köck, Jordi Teva, Jochen Kraft, Jörg Siegert, Franz Schrank, «Methods of simulating thin film deposition using spray pyrolysis techniques,» Microelectronic Engineering, vol. 117, pp. 57-66, 2014.

[24] Chen, Dong; Sharma, Sanjak K.; Mudhoo, Ackmez (2012): Handbook on Applications of ULTRASOUND. Sonochemistry for Sustainability. CRC Press 2012.

[25] Zhu, Guang; Lv, Tian; Pan, Liqun; Sun, Zhuo; Sun, Changqing (2011): All spray pyrolysis deposited CdS sensitized ZnO films for quantum dot-sensitized solar cells. Journal of Alloys and Compounds 509, 2011. 362-36

Chapter III : Films elaboration & results

III.1. ZnS thin films elaboration

III.1.1. Introduction

The first part of this chapter is dedicated to the description of the different experimental techniques used in this work. On a glass substrate, we deposit ZnS:Cd thin films form aqueous solution alcohol containing zinc chloride dehydrate ($ZnCl_2.2H_2O$) and thiourea ($CS(NH_2)_2$) in a volume of bidistilled water as a solvent on heated glass substrates using ultrasonic spray process. For doping we have used magnesium chloride dehydrate ($CdCl_2.\ 2H_2O$) with different percentage of: 0%, 2%, 4% and 6%.

III.2. Choice and preparation of substrate

In our work, the glass substrates used are equidistant (**Figure III.1**) that are sterilized by solvent solutions (distilled water, acetone, and ethanol) and dried with Joseph paper in the following steps:

Figure III.1. Isometric glass substrates and diamond pen.

- The glass substrates have cut into equal dimensional substrates by pen of diamond point(Figure II.9),
- Soak the substrates in acetone to remove grease and fats,
- The substrates are immersed in distilled water to remove traces of acetone,
- Soak the substrates in ethanol to remove the organic matter. The substrates are againimmersed in distilled water to remove traces ethanol,
- The glass slides ultrasonically cleaned in each for about 5 min,
- Drying the substrates using Joseph paper, so as not to leave any traces or impurities.

III.3. Preparation of precursor solutions

There are several precursors to obtain thin films of Zinc Sulfide, but in our work, we have chosen zinc acetate dihydrate and thiourea dissolved in aqueous alcohol solution; with molarity **C** equal to 0.1 mol/l. By following these steps:

- Measure a mass of zinc chloride dehydrate m = C.M.V using a balance (the molar mass M_{ZnCl_2} = 136.315 and $M_{CS(NH_2)_2}$ = 76.12);
- The previous mass was dissolved in an aqueous alcohol solution by volume V = 60ml;
- For doping we used magnesium chloride $CdCl_2.6H_2O$;
- The solution was stirred with ultrasonic bath cleaners for about five minutes.

III.4. Ultrasonic spray pyrolysis's equipment

We have developed zinc sulphide thin films using ultrasonic spray pyrolysis technique (**Figure III.2**), at laboratory of semiconductors of Annaba University.

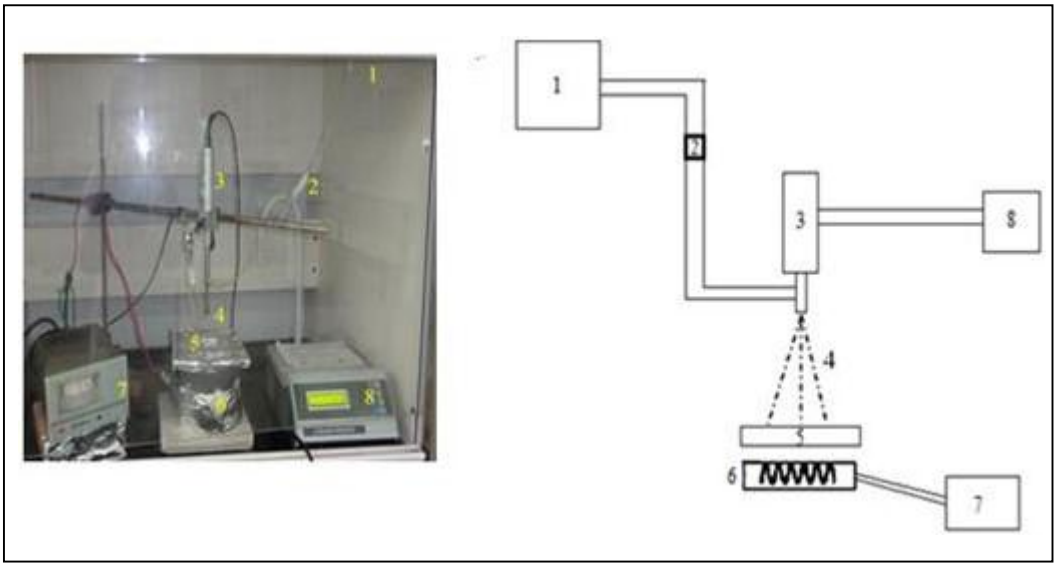

Figure III.2. Complete experimental devices of the ultrasonic spray pyrolysis technique.

The main elements of the experimental set up of the spray pyrolysis system are:

1. Ultrasonic generator (40 KHz): allows decomposing the solution at the atomizer to veryfine droplets (Ø ~40 µm);
2. Atomizer: the atomizer is placed on a support height adjustable to control the nozzlespray distance;
3. Substrate heater: it is substrate holder (Ø =25 cm) heated by joule effect.

III.5. Preparation of thin films

After preparing the substrates and solutions, all samples are preparation through thefollowing steps:

- The prepared solution with the molarity 0.1M by using methanol solvent is placed in asolution holder to be sprayed in the form of very thin drops, using ultrasonic generator, that precipitate over the glass substrate. Before deposition, the substrates were kept at ambienttemperature to avoid thermal shock.
- The substrates were heated to 450 °C temperature for each film.
- The nozzle was kept at a distance of 4.5 cm from the substrate during deposition.
- The spray rate was maintained at 60 ml/h using an ultrasonic generator (40 kHz).
- The spraying time (35 min) was maintained each time. When aerosol droplets came close to the substrates, the compounds reacted to become a new chemical compound ZnS.

Four samples have been prepared by changing the doping concentration: 0%, 2%, 4% and 6%. The used precursor for doping is Magnesium chloride

Table III.1: Process parameters for the spray deposition of ZnS thin films.

Precursor / molarity	**Zinc chloride ($ZnCl_2$) 0.1 mol/l**		**Thiourea ($SC(NH_2)_2$) 0.1 mol/l**	
Deposition time (min)	35			
Volume (ml)	60			
Nozzle-substrate distance (cm)	4.5			
Pression	Atmosphérique (1 atm)			
Substrate temperature (°C)	450			
Cd Dopant (%)	0	2	4	6

III.2.1. Results and discussion

III.2.1. Introduction

As commonly known, that the ZnS thin films properties are significant effected by technique of elaboration and deposition parameters. In the case of ultrasonic spray pyrolysis, the main parameter which is widely influenced on ZnS thin films properties is substrate temperature which controls the spices energy and motion onto substrate surface.

The purpose of this chapter is to present and interpret the experimental results of this work which aims the elaboration and characterization of zinc sulphide thin films deposited on glass substrates by ultrasonic spray pyrolysis technique at different Cd doping percentage (0, 2, 4 and 6 %).

III.2.2. Experimental details

ZnS thin films were prepared by spraying a solution contains a 0.1 mol/l of zinc chloride ($ZnCl_2.2H_2O$) and thiourea ($CS(NH_2)_2$) in a volume of bidistiled water as a solvent on heated glass substrates using ultrasonic spray process. The elaborated films were characterized in order to study their properties. The films structure was analyzed by X-ray diffraction using XPERT-PRO diffract meter. The optical transmittance spectra in UV–Visible rang was achieved using Perkin Elmer spectrophotometer. The electrical properties were studied using Hall effect method.

III.2.3. Structural properties

III.2.3.1. XRD analysis

The X-rays diffraction is carried out to study the crystalline quality of the un-doped and doped ZnS thin films elaborated at 350 °C substrate temperatures. **Figure IV.1** shows the XRD pattern of the samples. In all the films, the basic peaks were (100), (103), (10 10) and (10 12) planes were assigned to the 26.52°, 28.77°, 36.07° and 52.02°, respectively, according to the diffraction profiles (JCPDS Cad No. 039-1363).

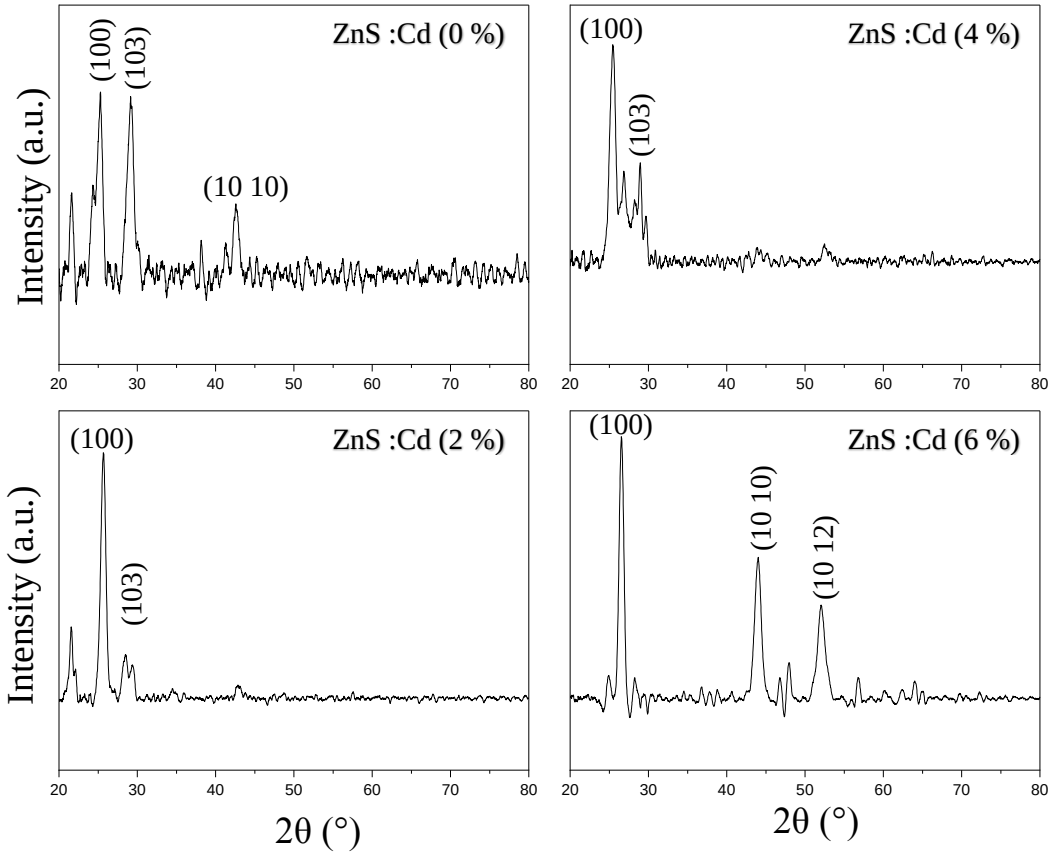

Figure III.3. XRD patterns of zinc sulfide as function of Cd doping.

Based on Figure III.3, we observe Cd doping peaks in films with low doping concentrations (Cd = 0% and 2%). However, these peaks disappear as the doping percentage increases to 4% and 6% in ZnS, indicating significant incorporation of dopant atoms into the material lattice.

X-ray diffraction (XRD) patterns confirm the formation of pure ZnS thin films across all deposited samples with varying doping levels. At Cd = 0%, a broad peak resembling a bump suggests the presence of an amorphous phase in the ZnS film. The crystalline structure of ZnS improves with Cd concentrations above 2%. This enhancement in crystallinity results from increased doping levels, facilitating the growth of the pure ZnS phase.

Doping cadmium (Cd) into zinc sulfide (ZnS) thin films can significantly influence their structural properties, primarily by altering the crystalline structure, lattice parameters, and defect formation. ZnS typically crystallizes in two major phases: cubic zinc blende (c-ZnS) and hexagonal wurtzite (h-ZnS). The incorporation of Cd can modify the phase preference due to changes in lattice

parameters and crystal growth kinetics.

Cd has a smaler ionic radius (Cd^{2+} ~ 78 pm) compared to Zn^{2+} (84 pm), which can lead to less lattice strain or distortions when substituted into the Zn sites of the ZnS lattice. This strain reduction can influence the crystallization process, potentially favoring the formation of a specific crystal phase (c-ZnS or h-ZnS) depending on the deposition conditions and Cd concentration [1].

Our findings show that increasing the temperature improved the crystallization of theZnS films.

III.2.3.2 Crystallite size, Microstrain and Dislocation

The crystallite size (D) represent the crystalline quality of the ZnS films. It wascalculated using the classical Scherrer formula [2, 3].

$$D = k.\lambda/\beta \cos\theta \qquad \text{(III.1)}$$

Microstrain (ε) of ZnS films was deduced by using the following equation [4, 5]:

$$\varepsilon = \frac{\beta \cos\theta}{4} \qquad \text{(III.2)}$$

Where λ is the X-ray wavelength of radiation, θ is the Bragg angle, β is FWHM calculated inradians. For the CuKa line, the shape factor k equal to 0.9.

Figure. III.4 represents the variation of crystallite size and strain versus the doping level. The crystallite size is calculated from the most intense diffraction peak for each sample.

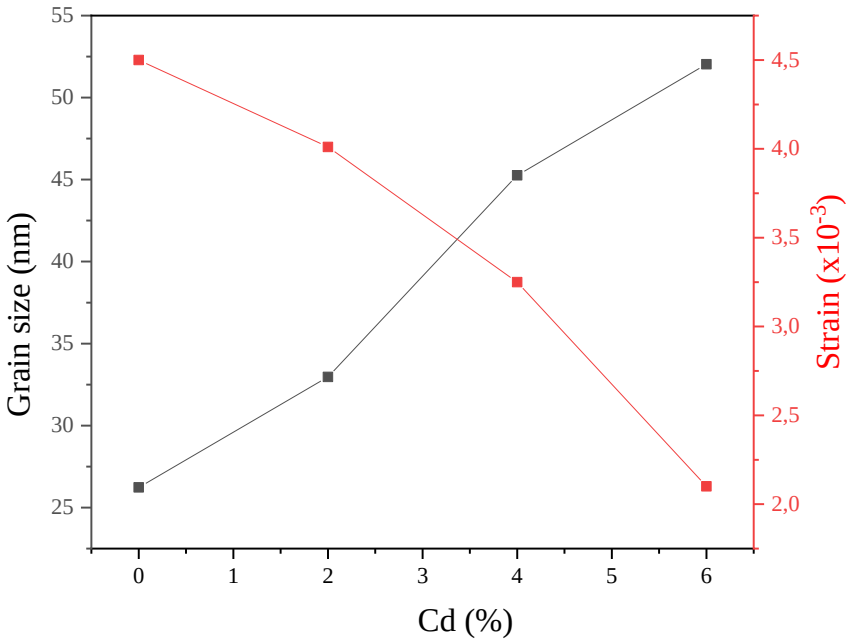

Figure III.4. Crystallite size and Microstrain of ZnS thin films as a function of Cd doping.

The increase in Cd concentration from 0% to 6% results in a notable increase in crystallite size, from 26.23 nm to 52.03 nm. Thus, the ZnS films prepared exhibit a nanocrystalline or nanostructured nature. Additionally, films deposited at higher doping level exhibit larger crystallites, which reduces strain and stress within the crystal lattice. This phenomenon contributes significantly to enhancing the crystallinity of the ZnS structure, as supported by the X-ray diffraction (XRD) spectra.

Increasing the doping level from 2% leads to an increase in crystallite size. This size increase is attributed to reduced lattice strain ε, which occurs due to a decrease in defect density within the films, resulting in network relaxation [6, 7]. This change can be attributed to the introduction of Cd, which introduces strain into the lattice due to the size difference between Cd^{2+} and Zn^{2+} ions. This strain significantly affects the mechanical stability and formation of defects within the thin film.

The third structural parameter analyzed is dislocation density. Dislocations are crystallographic defects or imperfections found within a crystal structure, impacting various material properties [8]. The density of dislocations was quantified using the formula [9, 10]:

$$\delta = \frac{1}{D^2} \qquad \text{(III.3)}$$

The variation of the dislocation density is shown in figure III.5.

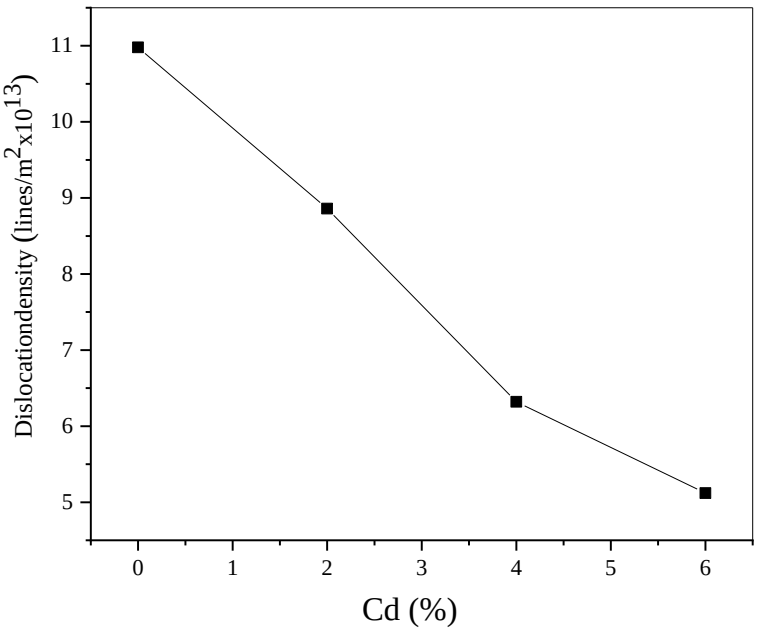

Figure III.5. Dislocation density of ZnS thin films versus the substrate temperature.

As the grain size increases, both microstrain and dislocation density decrease, suggesting an improvement in crystallinity. This relationship indicates that larger grains typically have fewer defects and internal stresses, resulting in a more ordered crystalline structure. Similar conclusions were reported in the study by Hasanzadeh [11, 12], reinforcing the understanding that grain size plays a crucial role in determining the structural integrity and quality of crystalline materials.

III.2.4. Optical properties

Transmitting spectrum of ZnS:Cd thin films were observed in the UV-visible ranges (300-800) nm and they are given in Figure III.6.

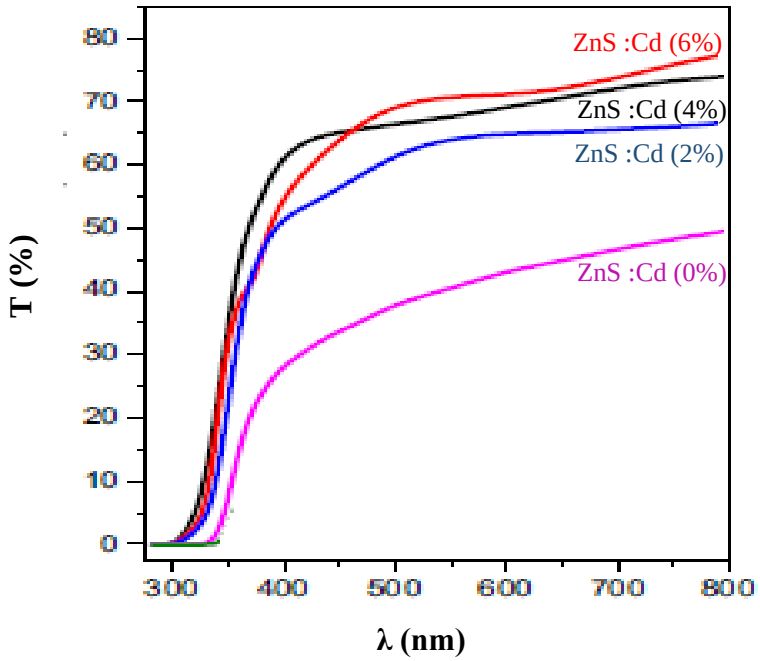

Figure III.6. Transmittance spectra of ZnS:Cd thin films.

The whole of the spectra of transmission obtained in our samples are composed of two regions: a region of strong absorption ($\lambda < 400$ nm), corresponding to fundamental absorption in thin films of ZnS. This absorption is due to the electronic transition inter band (the valence band and the band of conduction). The variation of the transmission in this region can be exploited for the determination of the optical band gap energy and the disorder. It was also observed that doping level has affected the position of absorption edge which shifted slightly to longer wavelength. The second region of strong transparency ($\lambda > 400$ nm): the value of the transmission is about 35% to 75%, in the wavelength range of 400–800 nm. This changing in transmission values is in good agreement with that obtained values (40–70%) by Daranfed et al. [13] on ZnS thin films prepared by ultrasonic spray method. It is noticed that the transmittance decrease with the increasing doping proportion, can be attributed to the film crystallinity improvement. We noticed that transmittance spectra have no interference fringe due to the incident light scattering in the material because of interface air/film roughness.

III.2.5. Electrical properties

For our study the resistivity is calculated by using Hall effect method. The variations of ZnS layers resistivity versus the doping level are presented in Fig. III.7.

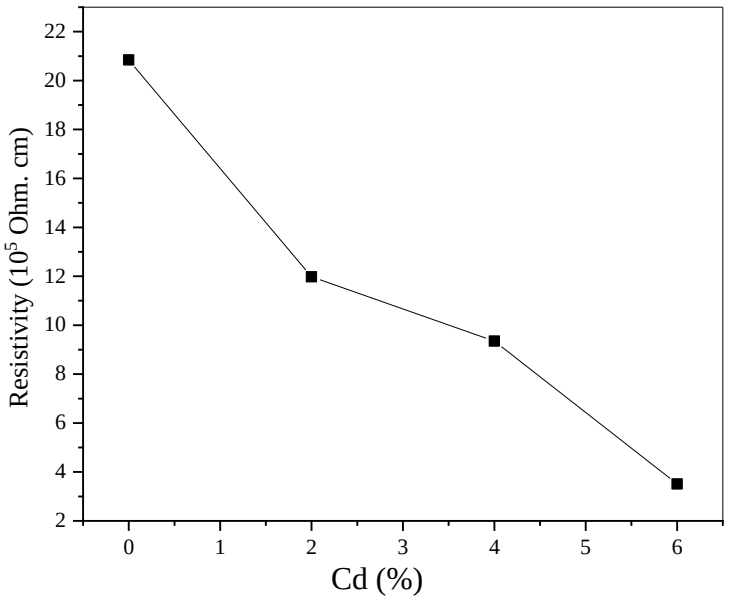

Figure III.7. Variation of the resistivity of ZnS:Cd thin films.

It could be observed that the resistivity of the grown films decreases from 20.84 $\times 10^5$ Ω.cm to 3.51 $\times 10^5$ Ω.cm with the increasing of the doping. These results are lower than Turan et al. ones [14], who studied the electrical properties of ZnO/Au/ZnS/Au films deposited by ultrasonic spray pyrolysis. Hence, the grain size enlargement leads to a decrease in grain boundary effects, because the boundary hinders the conduction mechanism of carriers charge, and this is the reason for a decrease in resistivity.

References

[1] Seyed Mostafa Mosavi, Hosein Kafashan, Physical properties of Cd-doped ZnS thin films, Superlattices and Microstructures, 126, 2019, 139-149. https://doi.org/10.1016/j.spmi.2018.12.002

[2] Hadi, E.H., Sabur, D.A., Chiad, S.S., Habubi, N.F., Abass, K.H., Journal of Green Engineering, 10 (10), 8390-8400 (2020).

[3] Hussin, H.A., Al-Hasnawy, R.S., Jasim, R.I., Habubi, N.F., Chiad, S.S., Journal of Green Engineering, 10(9) 7018-7028 (2020).

[4] Latif, D.M.A., Chiad, S.S., Erhayief, M.S., Abass, K.H., Habubi, N.F., Hussin, H.A., Journal of Physics, Conference Series 1003(1) 012108 (2018). https://doi.org/10.1088/1742-6596/1003/1/012108

[5] Othman, M.S., Mishjil, K.A., Rashid, H.G., Chiad, S.S., Habubi, N.F., Al-Baidhany, Journal of Materials Science: Materials in Electronics, 31(11), 9037-9043 (2020). https://doi.org/10.1007/s10854-020-03437-0

[6] Malle Krunks, Enn Mellikov, Thin Solid Films, 270, 1995, 33-36.

[7] P.R.Benger, K.Chang, P.Bhattacharya, J.Sing, K.K.Bajaj, Appl. Phys. Lett.53 (1988) 684– 686.

[8] G.K. Williamson, R.E. Smallman, Philosophical Magazine, 1, 34-45 (1956). https://doi.org/10.1080/14786435608238074

[9] Ali, R.S., Mohammed, S.A.A., Mohammed, A.H., IOP Conference Series: Materials Science and Engineering, 928(7), 072154 (2020). https://doi:10.1088/1757-899X/928/7/072154

[10]Sulaiman, H.T., Ali, R.S., Khoudhair, M.J., Mohammed, S.A.A. Neuro Quantologythis, 18(1), 99–10 (2020). https://doi:10.14704/nq.2020.18.1. NQ20113.

[11] J. Hasanzadeh, A. Taherkhani and M. Ghorbani, Chinese journal of physics, 51 (3), 2013, 540-550.

[12] A.S. Hasan, N. B. Hasan, A. J. Hayder, The first scientific conference for college of science, University of Karbala, 2013, 18-25.

[13] W. Daranfed, M.S. Aida, A. Hafdallah, H. Lekiket, Substrate temperature influence on ZnS thin films prepared by ultrasonic spray, Thin Solid Films 518(2009) 1082–1084.

[14] Evren Turan, Muhsin Zor, A. Senol Aybek, Metin Kul, Electrical properties of ZnO/Au/ZnS/Au films deposited by ultrasonic spray pyrolysis, Thin Solid Films 515 (2007) 8752–8755.

GENERAL CONCLUSION

This study involved the production of ZnS thin films using the ultrasonic spray pyrolysis technique, incorporating different levels of Cd doping (0%, 2%, 4%, and 6%). These films underwent comprehensive characterization to explore their characteristics. Structural analysis was conducted using X-ray diffraction via an XPERT-PRO diffractometer. Optical transmittance spectra within the UVVisible range were acquired using a Perkin Elmer spectrophotometer. Electrical properties were assessed using the Hall effect method employing HMS 3000 equipment. The main outcomes of this research can be summarized as follows:

- ✓ The ZnS film shows reflection from the planes (100), (103), (1010), and (1012) corresponding to angles of 26.52°, 28.77°, 36.07°, and 52.02°, respectively.- Increasing the doping level improved the crystallization of the ZnS:Cd films.
- ✓ The crystallite size increases with higher doping levels, ranging from 26.23 nm to 52.03 nm, resulting in reduced strain and stress within the crystal lattice of the films.
- ✓ The increase in crystallite size correlates with decreased lattice strain ε and dislocation density, attributed to a reduction in defect density within the films.
- ✓ The increase in transmittance of the films in the blue spectral range aligns well with findings in the literature.
- ✓ ZnS films exhibit promising results in terms of resistivity, which decreases with increasing doping levels